Progressive changes in sleep and its relations to amyloid-β distribution and learning in *App*$^{NL\text{-}G\text{-}F}$ mice

(*App*$^{NL\text{-}G\text{-}F}$ マウスにおける睡眠異常およびアミロイドβや記憶学習能力との関係についての解析)

2020

筑波大学グローバル教育院

School of the Integrative and Global Majors in University of Tsukuba

Ph.D. Program in Human Biology

Sakura Eri Bautista Maezono

筑　波　大　学

University of Tsukuba

博　士　（人間生物）　学　位　論　文

Ph.D. dissertation in Human Biology

Progressive changes in sleep and its relations to amyloid-β distribution and learning in App^{NL-G-F} mice

(*App*$^{NL-G-F}$ マウスにおける睡眠異常およびアミロイドβや記憶学習能力との関係についての解析)

2020

筑波大学グローバル教育院

School of the Integrative and Global Majors in University of Tsukuba

Ph.D. Program in Human Biology

Sakura Eri Bautista Maezono

Acknowledgement

I would like to express my utmost gratitude to my supportive and understanding research supervisor, Prof. Yu Hayashi, for his indispensable role in overseeing this project and guiding me every step of the way in completing this journey; yet, allowing me to grow as a researcher and as a person.

My sincerest appreciation goes to Prof. Masanori Sakaguchi for his continuous support and guidance, particularly in the behavioral part of my doctoral studies. Moreover, I am grateful to be under his supervision for the last six months of my doctoral studies.

I would like to extend my appreciation to Prof. Takashi Saito and Prof. Takaomi C. Saido for providing the Alzheimer's disease mouse model used in the study, $App^{NL\text{-}G\text{-}F}$ mice and their insights in carrying out my research paper.

I would also like to thank the rest of the collaborators, Ms. Mika Kanuka, Ms. Miho Morita, Ms. Chika Tatzusawa, and Dr. Taizo Kawano for providing technical assistance and expertise crucial to completing this project.

Special thanks to my dissertation committee, Prof. Michael Lazarus, Prof. Hiromasa Funato, and Prof. Tilo Kunath for their constructive feedbacks and discussions which help shape my doctoral studies starting from the 1st qualifying exam leading up to writing my thesis.

I am indebted to all the faculty members of the Human Biology Program and the SIGMA staff, for their continuous support and guidance during my doctoral studies.

I can’t thank my family enough, my husband, mother, grandmother, twin sister and little brother for their unconditional love, understanding and support throughout this Ph.D. journey.

To my son, Damon Mitchell Potter and his yet to be born sibling, you are both my inspiration. You are the source of my strength and resilience.

Table of Contents

Abstract

Patients with Alzheimer's disease often suffer from sleep disturbances. Alterations in sleep parameters, especially those related to rapid eye movement sleep, can precede the onset of dementia. Moreover, findings from recent animal studies provide strong support that insufficient sleep accelerates neurodegeneration. To accurately characterize the sleep impairments in patients with Alzheimer's disease and their underlying mechanisms using animal models, it is crucial to use models in which the same brain areas are affected in a manner similar to that observed in patients with the actual disease. Here, we focused on App^{NL-G-F} mice, in which expression levels and expression patterns of mutated amyloid precursor protein follow the endogenous patterns. We characterized the sleep architecture of the App^{NL-G-F} heterozygous and homozygous mice at two ages. At a younger age (6 months), the homozygous mice exhibited reduced rapid eye movement sleep. At an older age (12 months), the homozygous mice exhibited further reduction in rapid eye movement sleep together with a slight reduction in non-rapid eye movement sleep. By contrast, the sleep architecture of the heterozygous mice appeared overall normal at both ages. Furthermore, from the younger age, the homozygous mice exhibited a decrease in the ratio of electroencephalogram gamma power to delta power during rapid eye movement sleep, resembling the electroencephalogram slowing phenomenon observed in the preclinical or early stage of Alzheimer's disease. Thus, phenotypes related to rapid eye movement sleep exhibited by the homozygous mice resembled the features of preclinical or early stages of Alzheimer's disease. In addition, homozygous mice at both the younger and older ages showed learning and memory impairments in the trace fear conditioning task. Task performance strongly correlated with the amount of rapid eye movement sleep at the older age, but not at the younger age. Finally, measurements of

the amyloid-β accumulation in several brain areas revealed that amyloid-β accumulation in the pontine tegmental area and ventral medulla followed a course similar to that of the rapid eye movement sleep reduction, i.e., an age-dependent increase in the homozygous mice and low levels in the heterozygous mice. This is the first study to describe the sleep changes exhibited by $App^{NL\text{-}G\text{-}F}$ mice and the association of these sleep abnormalities with learning ability. This is also the first Alzheimer's disease mouse model to recapitulate EEG slowing during REMS appearing earlier than in wake as observed in patients with Alzheimer's disease.

Keywords: *Alzheimer's disease, knock-in mouse model, amyloid-β, rapid eye movement sleep, learning impairment*

Abbreviations

Aβ = Amyloid-β; APP = amyloid precursor protein; ChAT = choline acetyltransferase; CS = conditioned stimulus; EEG = electroencephalogram, EMG = electromyogram, FC = fear conditioning; MSDB = medial septum-diagonal band of Broca; NREMS = non-rapid eye movement sleep; OFT = open field test; PBS = phosphate-buffered saline; REMS = rapid eye movement sleep; TBS = Tris-buffered saline; US = unconditioned stimulus; WT = wild-type; ZT = zeitgeber time

List of Figures

List of Tables

Chapter 1: Introduction

1.1. Sleep states and functions

With a third of human life usually spent on sleeping, "Why do we sleep?" is a question that have perplexed many scientists. However, the answer remains elusive. Studies show that poor sleep negatively affects health. It is associated with mortality (Rod *et al.*, 2011), mental health (Zhang *et al.*, 2017), and neurodegenerative diseases (Malhotra, 2018), among many other illnesses and disorders.

Sleep can be further divided to two distinct stages: 1) Rapid eye movement sleep (REMS) and 2) Non-rapid eye movement sleep (NREMS). In humans, there are three NREMS stages and then followed by REMS. In rodents, simply separating sleep into their types based on the electroencephalogram (EEG) and electromyogram (EMG) recordings is currently the gold standard.

1.1.1 Rapid eye movement sleep (REMS)

REMS, also known as paradoxical sleep, is when there is increased brain activity, prominently fast, low amplitude neural oscillations (i.e. theta and gamma waves), coupled with muscle atonia during sleep. This type of sleep decreases with age (Floyd *et al.*, 2007). REMS has been suggested to be important for brain maturation in early life (Marks *et al.*, 1995). A more recent reported function of REMS is contextual memory consolidation linked to spatial and emotional memory (Boyce *et al.*, 2016). REMS behavioral disorder, characterized by acting out dreams and a lack of REMS atonia, is linked to neurodegenerative diseases (Zhou *et al.*, 2015). A study in humans has shown that shortened REMS and prolonged REMS latency are predictors of Alzheimer's disease and Dementia in general (Pase *et al.*, 2017).

Among the brain regions, previous studies have pointed that the brainstem plays a crucial role in the regulation of REMS (Sakai *et al.*, 2001; Boissard *et al.*, 2002; Lu *et al.*, 2006; Hayashi *et al.*, 2015; Weber *et al.*, 2015). Previous studies have also shown that acetylcholine release within the basal forebrain is highest during REMS, compared to NREMS and wake (Vazquez and Baghdoyan, 2001).

1.1.2 Non-rapid eye movement sleep (NREMS)

NREMS, also referred to as slow wave sleep (SWS), is the sleep state defined by slow, high amplitude oscillation (i.e. delta waves) and the presence of sleep spindles with low muscle tone. Some of the functions SWS has been implicated in are visuomotor and perceptual skill learning (Gais *et al.*, 2000; Huber *et al.*, 2004). In addition, the role of NREMS in brain maintenance via waste clearance are backed up by many studies (Xie *et al.*, 2013; Hablitz *et al.*, 2019; Lucey *et al.*, 2019).

Regulation and modulation of NREMS involve several brain regions including the basal forebrain, anterior hypothalamus, cerebellum, caudal brain stem, spinal cord and peripheral nerves (de Andrés *et al.*, 2011).

1.2. Sleep impairments and Alzheimer's disease

Alzheimer's disease is a slowly progressing neurodegenerative disease characterized by extracellular amyloid-β (Aβ) deposits, intracellular neurofibrillary tangles, and neuronal loss. In addition to cognitive impairments, sleep disturbances commonly occur in patients with Alzheimer's disease (Carpenter *et al.*, 1996; McCurry *et al.*, 1999). REMS deficit, for one, has been repeatedly observed in patients suffering from the said disease. Sleep impairments can exacerbate a decline in the quality of life, not only of the patients with Alzheimer's disease, but also that of the caregivers (Moran *et al.*, 2005). Moreover, recent studies in humans and animal models revealed that sleep

deprivation or fragmentation accelerates Aβ accumulation and may thus contribute to the progression of Alzheimer's disease (Kang *et al.*, 2009; Minakawa *et al.*, 2017; Shokri-Kojori *et al.*, 2018). This notion is further supported by recent findings that alterations in sleep are present before the onset of Alzheimer's disease (Ju *et al.*, 2013; Pase *et al.*, 2017).

Brain oscillatory activities are thought to play important roles in information processing and are altered in Alzheimer's disease and other neuronal diseases (Herrmann and Demiralp, 2005; Koenig *et al.*, 2005). An increase in delta power during REMS were observed in MCI and mild to moderate AD in previous human studies (Brayet et al., 2016; Petit et al., 1993). Another study about amnestic MCI patients, some of whom will likely develop AD, have shown alterations in the theta power during NREMS (Westerberg et al., 2012). An increase in delta power during resting awake state in mild probable Alzheimer's disease compared to control has been reported in the past as well (Coben *et al.*, 1983). Alterations in the oscillatory activities in Alzheimer's disease patients are most readily detected during REM sleep, with a decrease in high-frequency oscillations accompanied by an increase in low-frequency oscillations (Prinz *et al.*, 1992; Petit *et al.*, 1993). These alterations are also detected in subjects with mild cognitive impairment, suggesting that the alterations emerge from the preclinical stage of Alzheimer's disease (Brayet *et al.*, 2016).

1.3. Intrinsic problems of mouse models whose sleep have been characterized

In attempts to characterize the sleep disturbances accompanying Alzheimer's disease and to elucidate the underlying mechanisms, many studies have conducted sleep recordings in various mouse models of Alzheimer's disease (Jyoti *et al.*, 2010; Platt *et al.*, 2011; Roh *et al.*, 2012; Schneider *et al.*, 2014; Colby-Milley *et al.*, 2015; Sethi *et al.*,

2015; Kent *et al.*, 2018). The mouse models used in these studies, however, either carry multiple copies of *App* or *presenilin* or use heterologous promoters to express these genes, which likely leads to overexpression or ectopic expression of amyloid precursor protein (APP) or presenilin, factors that contribute to the generation of Aβ from APP. The phenotypes of such Alzheimer's disease mouse models may be due in part to an unintended consequence of the overexpression. Moreover, sleep/wake states are regulated by the interactions of various brain areas, and ectopic expression of APP or presenilin may affect such interactions and alter sleep in a largely different manner than in patients with the actual disease.

1.4 Selected Alzheimer's disease mouse model: $App^{NL\text{-}G\text{-}F}$

To overcome these concerns, we focused on the $App^{NL\text{-}G\text{-}F}$ mouse, a recently developed mouse model of Alzheimer's disease in which a mutated human version of *App* is singly knocked into the original *App* locus (Saito *et al.*, 2014). In these mice, the humanized *App* sequence contains three mutations that promote Aβ toxicity and are associated with familial Alzheimer's disease: the Swedish (NL), Beyreuther/Iberian (F), and Arctic (G) mutations. These mice do not exhibit elevated expression of APP, but do exhibit a progressive increase in the accumulation of Aβ, a higher ratio of Aβ42 to Aβ40, amyloidosis, and neuroinflammation in several brain areas (Saito *et al.*, 2014).

1.5 Objectives of the Study

To evaluate how the sleep architecture and state-dependent oscillatory brain activities are affected in $App^{NL\text{-}G\text{-}F}$ heterozygous and homozygous mice, we recorded the EEG and EMG from these mice at multiple ages. Furthermore, to gain insight into the brain areas responsible for the altered sleep patterns, Aβ accumulation was assessed in several subcortical areas involved in sleep regulation. In addition, to investigate the

relationship between the development of sleep disturbances and cognitive impairment, we assessed the learning and memory abilities in these mice and analyzed the correlation between their performance in the behavioral tasks and sleep parameters.

Chapter 2: Materials and Methods

2.1 Animals

Male and female $App^{NL\text{-}G\text{-}F/wt}$ mice on a C57BL/6J background were crossed to obtain male $App^{NL\text{-}G\text{-}F/wt}$, $App^{NL\text{-}G\text{-}F/NL\text{-}G\text{-}F}$, and control wild-type (WT) mice for analyses. The mice were group housed under a 12:12 h light-dark cycle (lights on at 9:00) under controlled temperature (23.5 ± 2.0°C) and humidity conditions (51.0 ± 10.0%) with free access to water and food. The mouse facility was SPF grade, and solid plastic cages (CLEA Japan, Inc., Japan) and paper chip bedding (Sankyo Labo Service Corp., Japan) were used. All animal experiments were approved by the Institutional Animal Care and Use Committee of the University of Tsukuba, and all procedures were conducted in accordance with the Regulations for Animal Experiments of the University of Tsukuba.

2.2 Behavioral tests

Male mice underwent the open field test (OFT) and trace fear conditioning (FC) test, which are described in detail below. Prior to each behavioral test, the mice were each handled for 4 days (2 min x 2 times on the first day and 2 min x 3 times for the next 3 days) according to a previous study (Purple *et al.*, 2017). The orders in which mice of different genotypes underwent behavioral experiments were randomized. During the experimental procedures and subsequent data analyses, the experimenter was blinded to the genotype.

2.2.1 Open field test

The OFT was performed as described in a previous study (Seibenhener and Wooten, 2015) with some modifications. Briefly, mice were individually placed in an acrylic box (40 x 40 x 40 cm) and the activity was monitored by a video camera positioned centrally above the box. Each session lasted 10 min per mouse and was performed between zeitgeber time (ZT) 3:00 and 5:00. Light intensity was fixed at

70 lx and white noise (80 dB) was applied. Video files were analyzed using the SMART Video Tracking software v3 (PanLab/Harvard Apparatus, Spain). The open field was divided into 16 equivalent square areas and the 4 inner squares were considered the central zone.

2.2.2 Trace fear conditioning

The trace FC test was performed as previously described (Chowdhury *et al.*, 2005; Purple *et al.*, 2017) with some modifications. On day 1, mice were trained between ZT 8:30 and 9:30. The training context (context A) was a chamber (31 x 24 x 21 cm) equipped with a stainless steel shock grid floor, as previously described (Arruda-Carvalho *et al.*, 2011). After 192 s in context A, each mouse received five sets of conditioned stimulus (CS)-unconditioned stimulus (US) pairs. The CS was a 20-s tone (~80 dB) and the US was a 2-s foot shock (0.75 mA). The CS and US were separated by a 10-s trace period. Between each set, there was a 180-s interval. Mice remained in the same context for an additional 180 s before being returned to their home cage. On day 2, a retrieval test was performed between ZT 6:00 and 8:00. Mice were placed in a novel environment (context B), which was an acrylic box (570 x 370 x 185 cm) wrapped outside with black paper sheets. After 192 s in context B, the CS was presented. During both the training and the retrieval test, mouse activity was monitored by a video camera to calculate the freezing rate. On day 1, the responsivity to the shock stimulus was assessed as described in our previous study (Purple *et al.*, 2017) with some modifications. Briefly, the distance of the mouse movement 2 s before and during the first shock presentation was measured using Freezeframe4 (Actimetrics Software, Wilmette, IL, USA), which digitized the video signal at approximately 10 Hz and allowed for measurement of the movement frame by frame.

Mice were judged as exhibiting freezing behavior if no movement except for that related to respiration was detected for at least 1 s by an experimenter blinded to the genotype.

2.3 EEG/EMG recording and analyses

Male mice were subjected to EEG/EMG recording to characterize the sleep architecture. To implant EEG and EMG electrodes, the mice were anaesthetized with isoflurane and placed in a stereotaxic frame (Leica Angle Two, Leica Microsystems Inc., Buffalo Groves, IL, USA). Core body temperature was maintained using a feedback-controlled heating pad. EEG electrodes were stainless steel recording screws implanted epidurally over the parietal cortex (3 mm posterior to bregma, 1.5 mm lateral to the midline) and cerebellum (6.5 mm posterior to bregma, 2 mm lateral to the midline). EMG electrodes were stainless steel Teflon-coated wires placed bilaterally into nuchal muscles. The electrodes were fixed to the skull with the resin cement (Super-Bond C&B set; Sun Medical, Japan). The mice were allowed to recover in their home cages for 2 weeks before being transferred to the sleep recording chambers. The mice were attached to the recording cables and acclimatized to the recording chamber for at least 5 days. Following 48 h of EEG/EMG recording under basal conditions, novel objects (marbles) were presented and EEG/EMG was recorded for an additional 4 h. The EEG/EMG data were amplified and filtered (band pass 0.5-250 Hz), digitized at a sampling rate of 512 Hz, and collected using VitalRecorder (Kissei Comtec, Japan).

The EEG signals were subjected to fast Fourier transform and further analysis using SleepSign (Kissei Comtec, Japan). The vigilance state in each epoch was manually classified as REMS, NREMS, or wakefulness, on the basis of the EEG patterns as well as the absolute delta (1-4 Hz) power, the theta (7-10 Hz) power to delta power ratio, the

absolute gamma (25-45 Hz) and the integral of the EMG signals (Supplementary Fig. 1). Epochs with high EMG and low delta power were classified as wakefulness. Epochs with high delta power and low EMG were classified as NREMS. Epochs with even lower EMG (suggestive of muscle atonia) and a high theta power to delta power ratio were classified as REMS. If a single epoch contained multiple states, the state with the highest occupancy was assigned. The epochs were 4 s long. For each mouse, the average EEG power spectrum of each vigilance state was calculated and normalized using the average absolute value of the total EEG power across all frequencies in every 4-sec epoch of the 24 h period across vigilance states. All manual scoring was performed by an experimenter blinded to the genotype.

2.4 Immunohistochemistry

Following transcardial perfusion with 0.1 M phosphate-buffered saline (PBS), dissected brains were post-fixed with 4% paraformaldehyde/PBS overnight, equilibrated with 30% sucrose/PBS, and sectioned at 40 μm using a microtome (Yamato Kohki, Japan). The sections were washed with distilled water and placed in 0.3% H_2O_2/MeOH for 30 min and washed with distilled water again. After washing with TBST (1xTBS (pH7.5) + 0.1% Tween20) and incubating for 30 min in Tris-NaCl-blocking buffer (1xTBS + 0.5% Blocking Reagent [Perkin Elmer, Waltham MA, USA; FP1020]), the sections were incubated with a primary antibody for choline acetyltransferase (ChAT; 1/100 goat anti-ChAT [EMD Millipore, Burlington, MA, USA; AB144P]) at room temperature overnight and washed three times with TBST. The sections were then incubated with a primary antibody for Aβ (1/1000 Mouse anti-human Aβ (N) (82E1) IgG [IBL; 10323]) at 4°C overnight. The sections were washed three times with TBST and incubated with secondary antibodies for ChAT (1/500 Donkey anti-goat IgG-Alexa 546

[Invitrogen Molecular Probes, Eugene, OR, USA; A-11056]) and Aβ (1/1000 Donkey anti-mouse horseradish peroxidase [Abcam, Cambridge, UK; ab7061]) combined with 1 μg/ml 4',6-diamidino-2-phenylindole for 120 min. After washing four times in TBST, the sections were incubated with fluorescein-tyramide reagent (Perkin Elmer; SAT701001KT) for 30 min and then washed four times in TBST. All sections were mounted on a slide glass using Immu-Mount (Thermo Scientific Shandon; 9990412). Images of the brain sections were obtained with a digital slide scanner (NanoZoomer XR, Hamamatsu Photonics, Japan). Quantification of Aβ-derived signals was performed as described in a previous study (DeVos *et al.*, 2018) with some modifications. Briefly, the regions of interest were set manually using a freehand selection tool by an experimenter blinded to the genotype. Images were then processed using an ImageJ-based algorithm (DeVos et al., 2018) with some modifications. For each individual mouse, the calculated mean plaque area from, typically, 3-4 coronal sections (at least 2 sections) was considered the plaque area for each brain region of that mouse. For the medial septum-diagonal band of Broca (MSDB), the ChAT-positive area was chosen within this region from coronal sections between bregma 1.10 mm and 0.62 mm. For the pons, the tegmental area dorsal to the motor trigeminal nucleus and ventral to the cuneiform nucleus in coronal slices between bregma -4.84 mm and -5.34 mm was selected. For the medulla, the area ventromedial to either the facial nucleus or the ambiguous nucleus in coronal slices between bregma -6.34 mm and -6.84 mm was selected.

2.5 Experimental design and statistical analysis

The experimenters performing the data analyses were blinded to the genotype when scoring or analyzing EEG/EMG, behavioral, or histological data. Statistical analyses were performed using SPSS (IBM Corp., Armonk, NY, USA), PRISM 8

(GraphPad Software, San Diego, CA, USA), or R statistical software (http://www.r-project.org/). Bar graphs and line graphs represent mean ± SEM. Each point on the bar graphs and scatter plots represents an individual mouse. For comparisons among three groups with multiple timepoints/trials, mixed ANOVA and post-hoc Games-Howell multiple comparison test were applied. Otherwise, Games-Howell multiple comparison test or Welch's t-test was applied for comparisons among three or two groups, respectively. For correlation analyses, Pearson's correlation coefficient (r) and the *P* value were calculated. Where applicable, all statistical tests were two-tailed. Significance was set at $P<0.05$. Details on sample sizes and results of statistical tests are described in Supplementary tables 1-7

2.6 Data availability

Data supporting the findings in this study are stored in a server at the University of Tsukuba and are available upon reasonable request.

Chapter 3: Results

3.1 Experimental timelines

To assess the sleep architecture, learning abilities, and Aβ plaque distribution in $App^{NL\text{-}G\text{-}F/wt}$ and $App^{NL\text{-}G\text{-}F/NL\text{-}G\text{-}F}$ mice at multiple ages, two independent mouse groups were subjected to experiments with different timelines. For each of the two groups, sleep recording was performed at 6 months or 12 months of age. After the sleep recording, trace FC was performed at 7 months or 13 months of age. When mice were further subjected to histological analyses, the mice were immediately killed by an overdose of anesthesia following trace FC to avoid any long-term effects of the fear experience.

3.2 Normal OFT performance and body weight in $App^{NL\text{-}G\text{-}F/wt}$ and $App^{NL\text{-}G\text{-}F/NL\text{-}G\text{-}F}$ mice

In addition, OFT was performed to evaluate anxiety and locomotor activity at 4 or 9 months (Supplementary Fig. 2). At neither age did heterozygous or homozygous mice display overt anxiety-like behavior, as reflected by a decrease in the time spent in the central zone (Supplementary Fig. 2A), or decreased locomotion according to the total distance travelled (Supplementary Fig. 2B). The body weight of heterozygous and homozygous mice also appeared equivalent to that of WT controls at all tested ages (Supplementary Fig. 3).

3.3 Progressive deterioration of sleep architecture in single *App* knock-in mice

The sleep architecture of $App^{NL\text{-}G\text{-}F/wt}$, $App^{NL\text{-}G\text{-}F/NL\text{-}G\text{-}F}$, and WT control mice was compared using 24-h recordings of EEG and EMG at either 6 or 12 months of age (Fig. 1).

3.3.1 Sleep architecture at a younger age

At 6 months, a reduction of the total time in REMS and in the REMS/total sleep ratio was detected in homozygous mice (Fig. 1C). This reduction in the total time spent in REMS was mostly attributed to changes in the light phase (resting phase) (Fig. 1A, D, E). A decrease in the number of wake and NREMS episodes was also observed (Fig. 1F). REMS latency, on the other hand, was not affected (Fig. 1H). The sleep architecture of heterozygous mice was grossly similar to that of the age-matched WT control mice T 6 months (Fig. 1).

3.3.2 Sleep architecture at an older age

At 12 months, a further reduction in the total time spent in REMS and the REMS/total sleep ratio was detected in the homozygous mice (Fig. 1C; REMS: $p = 6.76E-05$ and REMS/total sleep ratio: $p = 7.97E-05$) together with a shorter mean episode duration (Fig. 1G; REMS: $p = 0.009$ and REMS/total sleep ratio: $p = 0.0005$). Again, the reduction in the total time spent in REMS was mostly attributed to changes in the light phase (Fig. 1B, D, E). In addition, a decrease in the total time spent in NREMS and an increase in the total time spent awake was observed at this age (Fig. 1C). In contrast to REMS, the change in the amount of wake and NREMS seemed to arise from changes in the dark phase (active phase) (Fig. 1D, E). For the wake state, the mean episode duration was increased, whereas for NREMS, the number of episodes was decreased (Fig. 1F, G). REMS latency was not affected even at 12 months (Fig. 1H). The sleep architecture of heterozygous mice was not significantly different to that of the age-matched WT control mice at 12 months (Fig. 1).

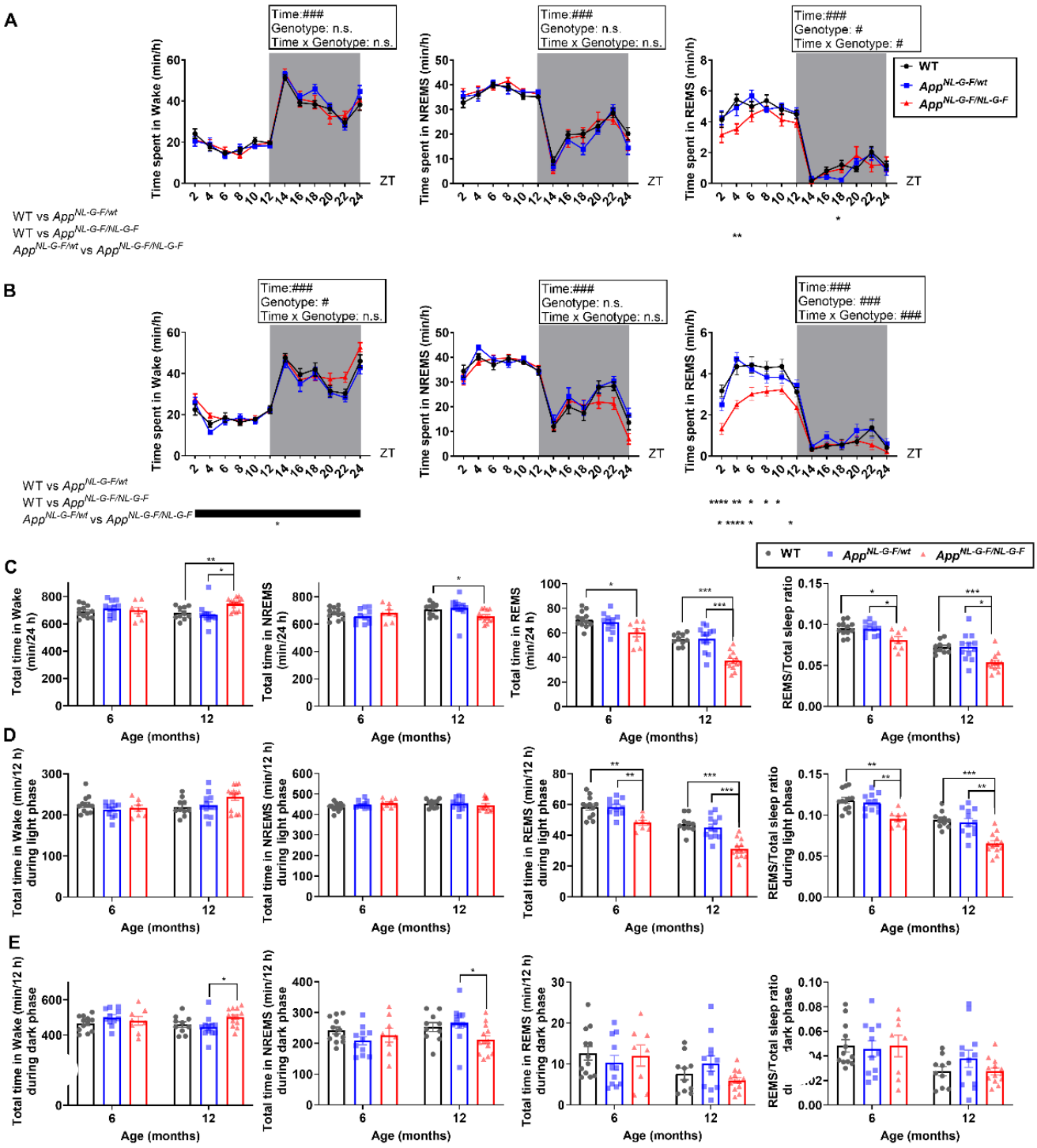
A
Time:###
Genotype: n.s.
Time x Genotype: n.s.
Time spent in Wake (min/h)
Time spent in NREMS (min/h)
Time:###
Genotype: #
Time x Genotype: #
Time spent in REMS (min/h)
ZT
WT
App NL-G-F/wt
App NL-G-F/NL-G-F
WT vs App NL-G-F/wt
WT vs App NL-G-F/NL-G-F
App NL-G-F/wt vs App NL-G-F/NL-G-F
B
Time:###
Genotype: #
Time x Genotype: n.s.
Time:###
Genotype: n.s.
Time x Genotype: n.s.
Time:###
Genotype: ###
Time x Genotype: ###
C
Total time in Wake (min/24 h)
Total time in NREMS (min/24 h)
Total time in REMS (min/24 h)
REMS/Total sleep ratio
Age (months)
D
Total time in Wake (min/12 h) during light phase
Total time in NREMS (min/12 h) during light phase
Total time in REMS (min/12 h) during light phase
REMS/Total sleep ratio during light phase
E
Total time in Wake (min/12 h) during dark phase
Total time in NREMS (min/12 h) during dark phase
Total time in REMS (min/12 h) during dark phase
REMS/Total sleep ratio during dark phase

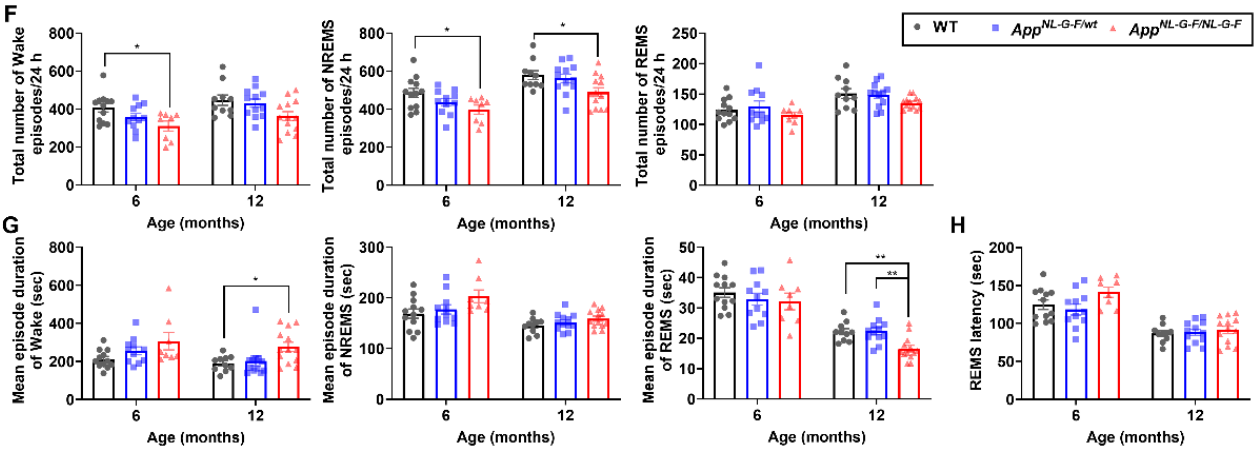

Figure 1. *App*$^{NL\text{-}G\text{-}F/NL\text{-}G\text{-}F}$ mice exhibit age-dependent impairments in sleep architecture.

(A and B) Diurnal sleep-wake cycles of 6-month-old **[A]** and 12-month-old **[B]** mice. Each point represents the mean ± SEM. #*P*<0.05, ###*P*<0.001, mixed ANOVA. **P*<0.05, ***P*<0.01, ****P*<0.001, *****P*<0.0001, post-hoc Games-Howell multiple comparison test. **(C-E)** Total amount of wake, NREMS, REMS, and ratio of REMS to total sleep (24 h **[C]**, light period **[D]**, and dark period **[E]**). **(F and G)** Number of episodes **[F]** and mean episode duration **[G]** in each stage of wake, NREMS, and REMS. **(H)** REMS latency. Bar graphs represent the mean ± SEM. Each point represents an individual mouse. **P*<0.05, ***P*<0.01, ****P*<0.001, Games-Howell multiple comparison test. Detailed results of the statistical tests are described in Supplementary Table 1.

3.4 Alterations of brain oscillatory activities during sleep in single *App* knock-in mice

The brain exhibits oscillatory activities across various frequencies with distinct patterns depending on the vigilance state. Such oscillatory activities are thought to play important roles in information processing and are altered in many neuronal diseases, including Alzheimer's disease, with distinct characteristics depending on the disease

(Herrmann and Demiralp, 2005; Koenig *et al.*, 2005). In Alzheimer's disease, alterations in the oscillatory activities are most readily detected during REM sleep, with a decrease in high-frequency oscillations accompanied by an increase in low-frequency oscillations (Prinz *et al.*, 1992; Petit *et al.*, 1993). These alterations are also detected in subjects with mild cognitive impairment, suggesting that the alterations emerge from the preclinical stage of Alzheimer's disease (Brayet *et al.*, 2016).

To investigate whether brain oscillatory changes occur in $App^{NL\text{-}G\text{-}F/wt}$ and $App^{NL\text{-}G\text{-}F/NL\text{-}G\text{-}F}$ mice, the power spectra of EEG obtained at different vigilance states were compared between genotypes at 6 and 12 months (Fig. 2).

3.4.1 Brain oscillatory activities during sleep at a younger age

At 6 months, the homozygous mice had a significantly higher delta power during REMS compared with WT, whereas the delta power during NREMS was not affected (Fig. 2D, E). By contrast, during NREMS, theta power was significantly lower in the homozygous mice (Fig. 2G). For both sleep stages at 6 months, although not significant, there was a trend toward decreased gamma power in the homozygous mice (Fig. 2J, K).

3.4.2 Brain oscillatory activities during sleep an older age

At 12 months, the oscillatory activity during sleep was further affected in the homozygous mice. During both sleep stages, delta power was significantly increased, whereas theta and gamma power were significantly decreased (Fig. 2D, E, G, H, J, K).

3.4.3 Brain oscillatory activities during wake at both ages

Oscillatory activity during the wake state was less affected in the homozygous mice. Theta and gamma power appeared normal at both ages, whereas delta power was increased (Fig. 2C, F, I)

3.4.4 Fast/slow oscillatory power in the different stages of the sleep-wake cycle

Considering the reported decrease in high-frequency oscillations and the increase in low-frequency oscillations in patients with early Alzheimer's disease, we next compared the ratio of fast oscillatory (gamma) power to slow oscillatory (delta) power. The ratio was significantly lower during REMS in the homozygous mice at 6 months, when the ratio appeared unaffected during wake or NREMS (Fig. 2L, M, N). In addition, the ratio of theta power to delta power during REMS was reduced in the homozygous mice (Fig. 2O).

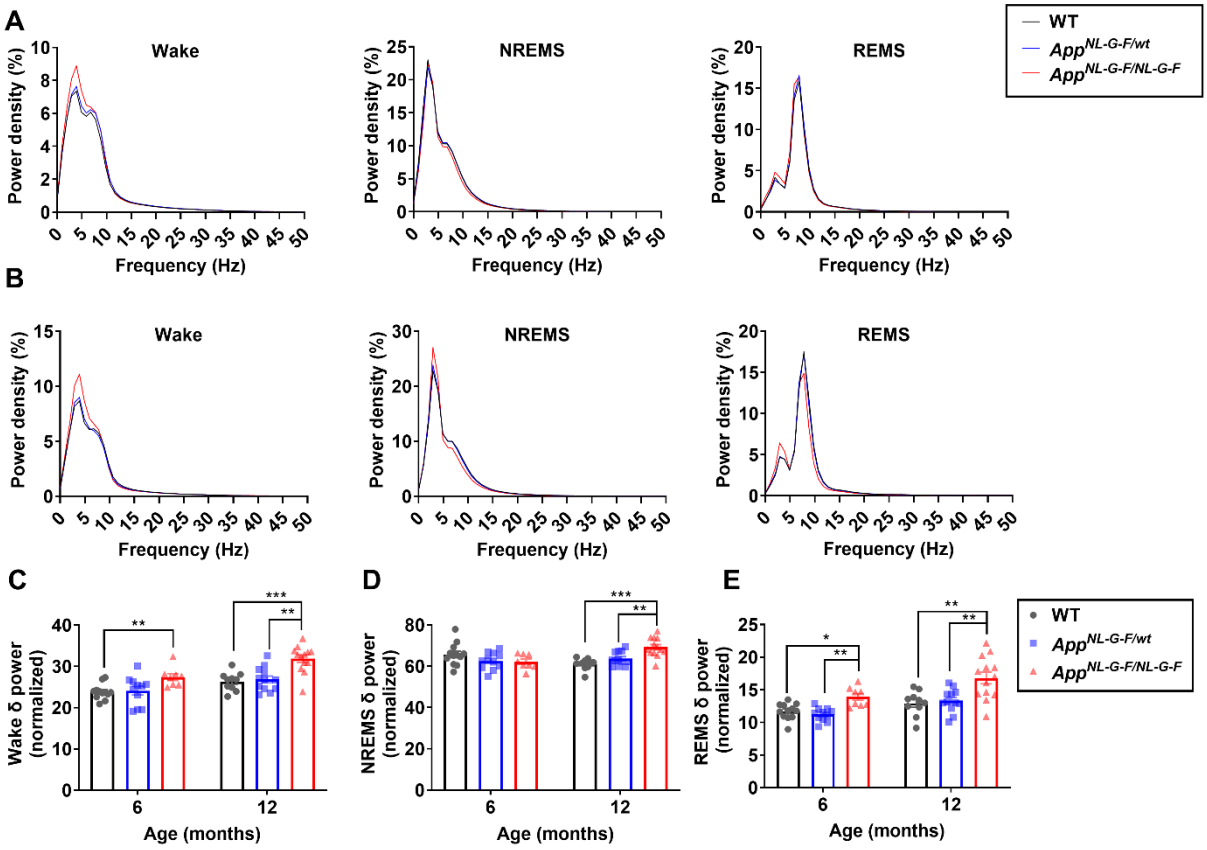

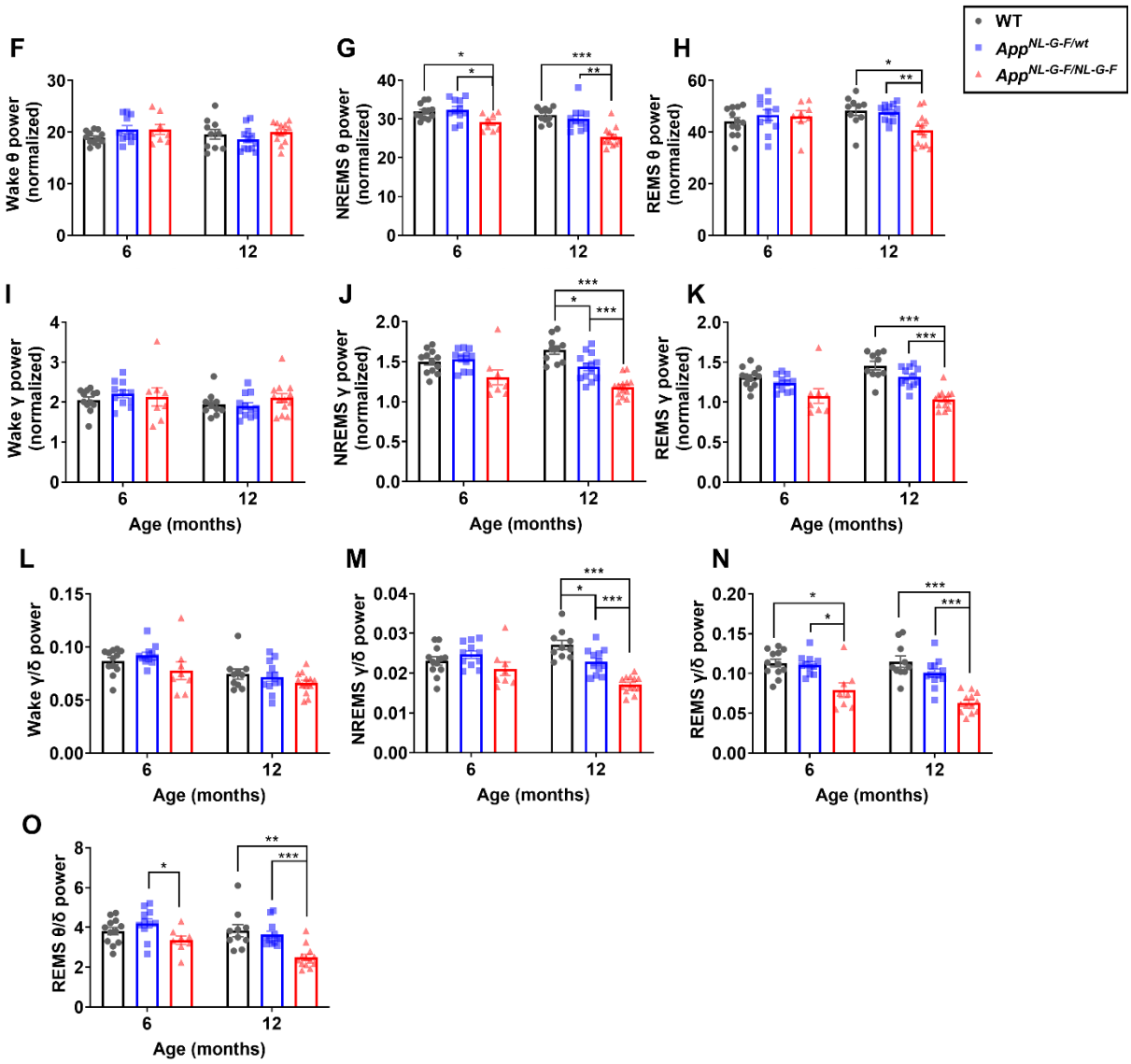

Figure 2. *App*$^{NL\text{-}G\text{-}F/NL\text{-}G\text{-}F}$ mice exhibit age-dependent alterations in brain oscillatory activities.

(A and B) EEG power spectrum of wakefulness, NREMS, and REMS in 6-month-old **[A]** and 12-month-old **[B]** mice. **(C-K)** Comparison of delta (δ; 1-4 Hz) power **[C-E]**, theta (θ; 7-10 Hz) power **[F-H]**, and gamma (γ; 25-45 Hz) power **[I-K]** during wake **[C, F, I]**, NREMS **[D, G, J]**, and REMS **[E, H, K]**. **(L-N)** Ratio of gamma to delta power during wake **[L]**, NREMS **[M]**, and REMS **[N]**. **(O)** Ratio of theta to delta power during REMS. Bar graphs represent mean ± SEM. Each point represents an individual mouse.

*P<0.05, **P<0.01, ***P<0.001, Games-Howell multiple comparison test. Detailed results of the statistical tests are described in Supplementary Table 2.

3.5 Sleep under novel object presentation

Human sleep is often affected by external stimuli. Exposing rodents to novel objects also affect their sleep (Schiffelholz and Aldenhoff, 2002). Therefore, we next examined how the presentation of novel objects affected sleep in $App^{NL\text{-}G\text{-}F/wt}$ and $App^{NL\text{-}G\text{-}F/NL\text{-}G\text{-}F}$ mice. Sleep was recorded from these mice and WT control mice for 4 h upon exposure to novel objects at 6 and 12 months (Fig. 3).

At both ages, similar to undisturbed sleep, the REMS/total sleep ratio was reduced in the homozygous mice (Fig. 3A). In addition, the REMS latency was decreased in the homozygous mice at 6 months (Fig. 3C). Thus, under specific conditions, the first episode of NREMS was shortened in these mice.

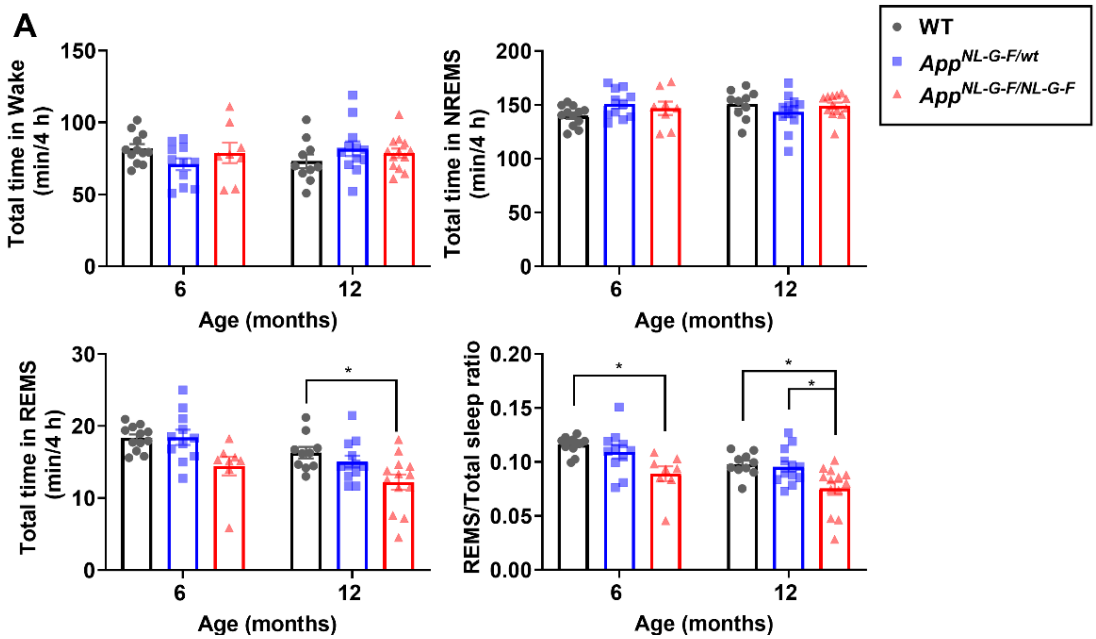

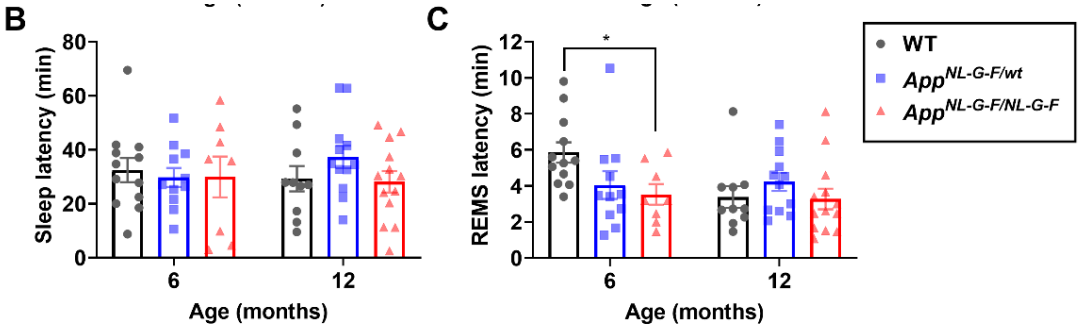

Figure 3. *App*$^{NL\text{-}G\text{-}F/NL\text{-}G\text{-}F}$ mice exhibit reduced REMS following exposure to novel objects.

(A) Total amount of wake, NREMS, REMS, and ratio of REMS to total sleep following presentation of novel objects. **(B and C)** Latency to sleep **[B]** or REMS **[C]** following presentation of novel objects. **P*<0.05, Games-Howell multiple comparison test. Bar graphs represent mean ± SEM. Each point represents an individual mouse. Detailed results of the statistical tests are described in Supplementary Table 3.

3.6 Learning and memory impairment in single *App* knock-in mice is associated with REMS deficits

Both sleep impairment and cognitive decline are commonly associated with the clinical stage of Alzheimer's disease (Carpenter *et al.*, 1996; McCurry *et al.*, 1999; Liguori *et al.*, 2014). The *App*$^{NL\text{-}G\text{-}F/NL\text{-}G\text{-}F}$ mice exhibited various age-dependent sleep deficits, especially in REMS. Here, we addressed whether the detected REMS defects were associated with learning and memory impairments. To investigate the correlation between sleep parameters and learning and memory performance at the individual level, the mice used in the sleep study were also subjected to a learning task. The FC task is a commonly used memory task in which an aversive US (foot-shock) is associated with some CS, typically a visual or an auditory cue. *App*$^{NL\text{-}G\text{-}F/NL\text{-}G\text{-}F}$ mice are reported to perform normally in a contextual FC protocol, even at 15-18 months of age (Sakakibara

et al., 2018). Here, we focused on trace FC. The trace FC is another hippocampus-dependent learning paradigm (McEchron *et al.*, 1998; Quinn *et al.*, 2002) that assesses temporal associative memory. In trace FC, a temporal gap is set between the CS (auditory tone) and the US (Huerta *et al.*, 2000; Misane *et al.*, 2005). Association of the temporally separated CS and US requires brain areas that are not essential for the delay FC (in which there is no gap between the CS and US), including the hippocampus and the prefrontal cortex (Gilmartin and Helmstetter, 2010). On day 1, the CS followed by the US was administered five times to mice at either 7 or 13 months of age. Importantly, in all genotypes, the first US evoked a similar increase in movement, indicating that the sensitivity to the US itself was unaltered (Fig. 4A).

3.6.1 Memory impairment at a younger age

At 7 months, both the heterozygous and homozygous mice normally learned the association between the CS and US on day 1, as assessed by a gradual increase in the freezing rate during the CS (Fig. 4B). On day 2, the freezing rate following exposure to the tone was reduced in the homozygous mice compared to the WT control mice, suggesting impaired retention or recall of the memory (Fig. 4C).

3.6.2 Learning impairment at an older age

At 13 months, the homozygous mice, and to a lesser extent the heterozygous mice, exhibited learning impairment on day 1 compared with the WT control (Fig. 4B). The homozygous mice also exhibited a trend toward a reduction in the freezing rate on day 2 (Fig. 4C).

3.6.3 Correlation between REMS parameters and cognitive function

To address whether the learning and memory deficits were associated with the sleep abnormalities, we performed correlation analyses between various sleep

parameters and the freezing rate in the trace FC test. The freezing rate during the third CS on day 1, which was reduced in the 13-month-old homozygous mice and had apparently not yet reached a plateau in the WT control mice, strongly and positively correlated with the total time in REMS (Fig. 4E). A similar trend was observed for the freezing rate on day 2 (Fig. 4G). By contrast, in the 7-month-old mice, although deficits in both REMS and trace FC were observed in the homozygous mice, no significant correlation was detected between the freezing rates and any sleep parameters tested, suggesting a specific correlation of the learning ability with REMS duration at the older age (Fig. 4D, F, Supplementary Fig. 4). We detected no significant correlation between the freezing rates and any sleep parameters tested in $App^{NL\text{-}G\text{-}F/wt}$ or WT mice (Supplementary Fig. 4).

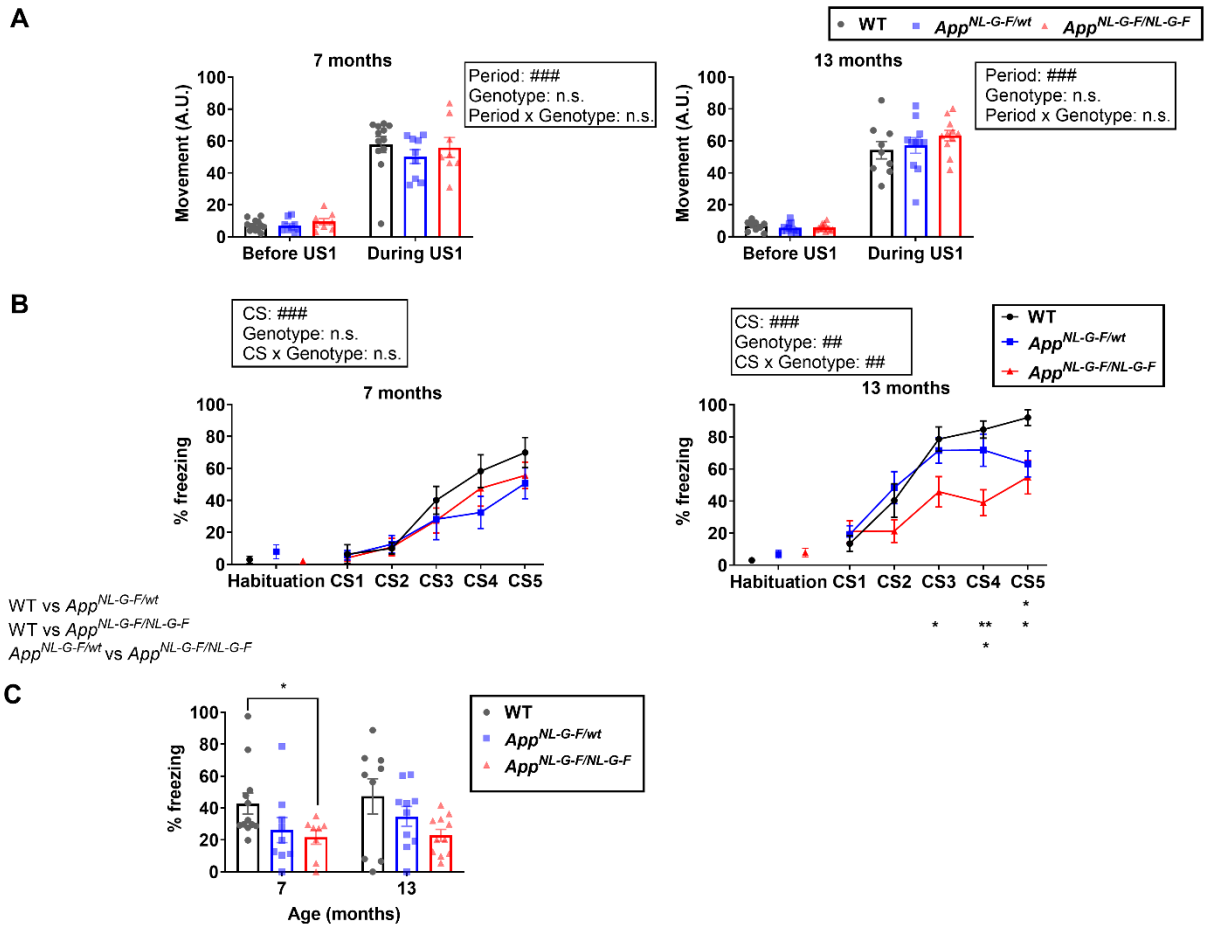

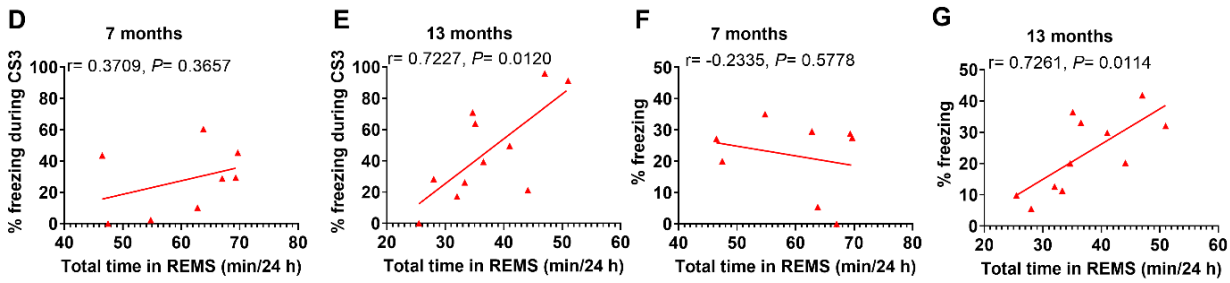

Figure 4. Impaired performance of *App*$^{NL\text{-}G\text{-}F/NL\text{-}G\text{-}F}$ mice in trace FC and its correlation with the amount of REMS.

(A) Movement of each 7-month-old and 13-month-old mouse before and during the first US. ###*P*<0.001, mixed ANOVA. **(B)** Percent time spent freezing during habituation or CS on day 1 (training). Each point represents mean ± SEM. ##*P*<0.01, ###*P*<0.001, mixed ANOVA. **P*<0.05, ***P*<0.01, post-hoc Games-Howell multiple comparison test. **(C)** Percent time spent freezing during CS on day 2 (retrieval). Bar graphs represent the mean ± SEM. Each point represents an individual mouse. **P*<0.05, Games-Howell multiple comparison test. **(D and E)** Correlation between the total amount of REMS and the percent time spent freezing during the third CS on day 1 (training) in younger **[D]** and older **[E]** *App*$^{NL\text{-}G\text{-}F/NL\text{-}G\text{-}F}$ mice. **(F and G)** Correlation between the total amount of REMS and the percent time spent freezing during CS on day 2 (retrieval) in younger **[F]** and older **[G]** *App*$^{NL\text{-}G\text{-}F/NL\text{-}G\text{-}F}$ mice. Each point represents an individual mouse. Pearson's correlation coefficient (r) and *P* value are provided. Detailed results of the statistical tests are described in Supplementary Table 4.

3.7 Accumulation of Aβ in brain regions involved in REMS regulation

Amyloidosis does not proceed in a uniform manner across all brain areas. One critical advantage of the Alzheimer's disease mouse model used in this study is that the *App* expression is predicted to faithfully recapitulate the endogenous pattern (Sasaguri *et*

al., 2017). Thus, we next addressed Aβ accumulation in brain areas related to REMS in these mice.

3.7.1 Aβ accumulation in the forebrain

First, consistent with previous reports (Saito *et al.*, 2014; Whyte *et al.*, 2018), Aβ accumulation in the hippocampus and cortex increased with age in both the homozygous and heterozygous mice (Fig. 5C, D, J, K). The basal forebrain cholinergic neurons contribute to sleep-wake regulation and are well known to be damaged in Alzheimer's disease (Whitehouse *et al.*, 1981, 1982; Lee *et al.*, 2005; Ozen Irmak and de Lecea, 2014; Xu *et al.*, 2015). Among these neurons, cholinergic neurons in the MSDB project to the hippocampus and are involved in oscillatory activity, neurogenesis, and learning and memory (Yoder and Pang, 2005; Hasselmo, 2006; Zhu *et al.*, 2017). Aβ accumulation in the MSDB also appeared to progress in a manner different from that in the hippocampus or cortex, with comparable levels in the homozygous mice at 7 months and 13 months and in the heterozygous mice at 13 months (Fig. 5A-D, I-K).

3.7.2 Aβ accumulation in the brainstem

The major sleep defect detected in the current study occurred during REMS. Many studies describe a crucial role of the brainstem in REMS regulation, especially the pontine tegmental area and the ventral medulla (Sakai *et al.*, 2001; Boissard *et al.*, 2002; Lu *et al.*, 2006; Hayashi *et al.*, 2015; Weber *et al.*, 2015).

Aβ seemed to accumulate in these brainstem areas in a manner different from that in the hippocampus and cortex. In these areas, Aβ accumulation largely increased from 7 months to 13 months in the homozygous mice, whereas it was hardly

detectable in the heterozygous mice, a pattern that somewhat resembled the progression of the REMS impairment (Fig. 5E-H, L, M).

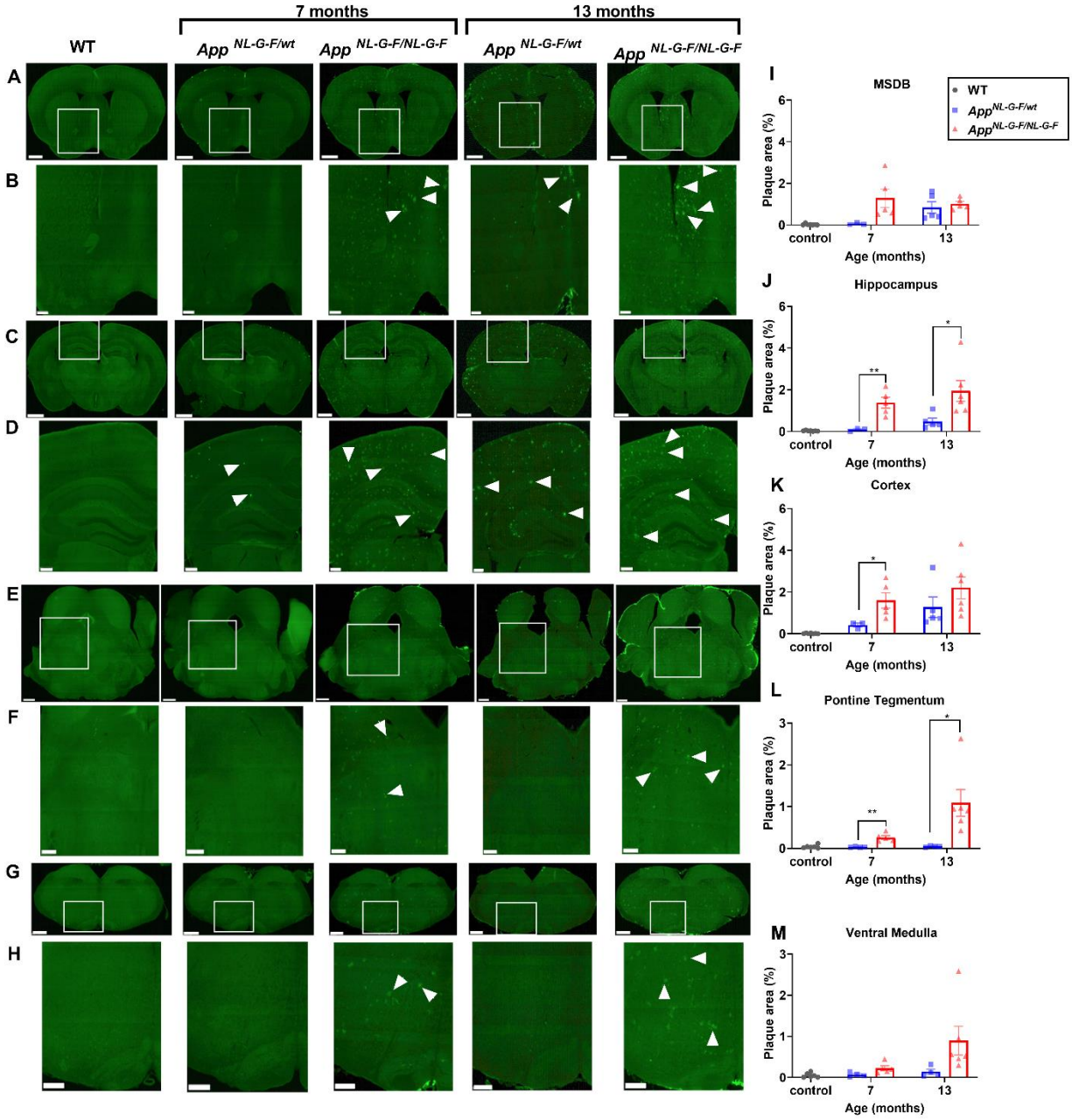

Figure 5. Aβ deposition in brain areas related to REMS regulation in *App*$^{NL\text{-}G\text{-}F/wt}$ and *App*$^{NL\text{-}G\text{-}F/NL\text{-}G\text{-}F}$ mice.

(A-H) Representative images of brain sections immunostained for Aβ. Images in **B, D, F, and H** are higher magnifications of the areas enclosed in **A, C, E, and G**. Sections

contain the following brain regions: MSDB **[A, B],** hippocampus and cortex **[C, D]**, pontine tegmental area **[E, F]**, and ventral medulla **[G, H]**. Scale bar: 2.5 mm **[A, C, E and G]**, 1.0 mm **[B, D, F and H]**. **(I-M)** Quantification of Aβ plaque (bright green) areas in MSDB **[I]**, hippocampus **[J]**, cortex **[K]**, pontine tegmental area **[L]**, and ventral medulla **[M]**. Bar graphs represent the mean ± SEM. Each point represents an individual mouse. **P*<0.05, ***P*<0.01, Welch's t-test. Detailed results of the statistical tests are described in Supplementary Table 5.

Chapter 4: Discussion

4.1 Significance of the Study

This is the first study to describe the sleep abnormalities exhibited by $App^{NL\text{-}G\text{-}F}$ homozygous and heterozygous mice and the association of these sleep abnormalities with learning ability. Sleep is regulated by various brain areas and neuronal subtypes. Thus, addressing the association between sleep and Alzheimer's disease using mouse models that overexpress or ectopically express APP or presenilin could complicate interpretations. Unlike previous studies in which the applied mouse models carried either multiple copies of *App* or *presenilin* or use heterologous promoters to express these genes, the present study used a mouse model in which mutated *App* was singly knocked into the original *App* locus. Indeed, homozygous mice faithfully recapitulated several aspects of the sleep abnormalities associated with preclinical or early Alzheimer's disease.

4.2 Changes in REMS as an early emerging phenotype, consistent with human studies

First, the amount of REMS was decreased from an early age when no changes in the amount of wake or NREMS were detected. This is consistent with a recent prospective study in humans showing that the reduction in the total time spent in REMS, but not in NREMS, is associated with a higher risk for Alzheimer's disease (Pase *et al.*, 2017). Second, during REMS, slow oscillatory activity (1-4 Hz) was increased while fast oscillatory activity (25-45 Hz) was decreased. Again, studies of patients with early-stage Alzheimer's disease or mild cognitive impairment report a similar shift in oscillatory activity during REMS (Prinz *et al.*, 1992; Petit *et al.*, 1993; Brayet *et al.*, 2016)). Thus, we believe the $App^{NL\text{-}G\text{-}F}$ knock-in mouse is highly useful for elucidating the mechanisms underlying sleep deficits in Alzheimer's disease.

4.3 Aβ accumulation in the brainstem as a critical factor in developing sleep deficits in Alzheimer's disease

The sleep architecture in the homozygous mice at 6 months of age was characterized by a decrease in REMS. At 12 months of age, the reduction of REMS was further pronounced, and NREMS was also reduced. By contrast, the sleep architecture of the heterozygous mice appeared mostly normal, even at 12 months of age. This might be explained by the time course of Aβ accumulation in brain areas crucial for REM sleep regulation. Accumulating evidence supports an essential role of the pontine tegmental area and ventral medulla in regulating REMS (Sakai *et al.*, 2001; Boissard *et al.*, 2002; Lu *et al.*, 2006; Hayashi *et al.*, 2015; Weber *et al.*, 2015). In these two areas, in contrast to the hippocampus or cortex, Aβ was almost undetectable in the heterozygous mice. On the other hand, in the homozygous mice, Aβ in these two areas increased with age, consistent with the progressive decrease in REMS. Therefore, damage to the brainstem might be critical for the development of sleep deficits in Alzheimer's disease. Recent studies also point to the roles of these areas in regulating NREMS, which might account for the decrease in NREMS at later stages (Anaclet *et al.*, 2014; Hayashi *et al.*, 2015). The basal forebrain cholinergic neurons are commonly damaged in Alzheimer's disease and are involved in sleep-wake regulation (Whitehouse *et al.*, 1981, 1982; Lee *et al.*, 2005; Ozen Irmak and de Lecea, 2014; Xu *et al.*, 2015).The time course of the Aβ accumulation in the MSDB of the basal forebrain, which contains many cholinergic neurons projecting to the hippocampus, in both the heterozygous and homozygous mice appeared not to be strongly correlated with the progression in sleep impairment. In addition to the brainstem and MSDB, various brain areas, including the hypothalamus

and midbrain, are involved in sleep regulation. Further studies are required to determine damage to which neurons largely contributes to the sleep deficits.

4.4 Limitations of the Study

While the reduction in REMS at the younger age in the homozygous mice was consistent with human studies on preclinical or early stages of Alzheimer's disease (Prinz *et al.*, 1982; Pase *et al.*, 2017), the reduction in the ratio of deep NREMS (stage 3 or 4), which is especially prominent in the advanced stages of Alzheimer's disease (Prinz *et al.*, 1982), was not obvious in the homozygous mice. The homozygous mice rather exhibited increased delta power, although the total amount of NREMS was reduced. Thus, the homozygous mice, although an excellent model for preclinical or early stages of Alzheimer's disease, might not recapitulate the sleep impairments that emerge in the advanced stages of the disease. In addition, there are also reports that patients with mild cognitive impairment, part of which will likely develop Alzheimer's disease, exhibit reduction in the time spent in both REMS and deep NREMS (Prinz *et al.*, 1982), suggesting that sleep impairments accompanying Alzheimer's disease are not uniform. It would be interesting to evaluate the relation between sleep impairment and the accumulation of Aβ in the pontine tegmental area and ventral medulla in patients with various stages of Alzheimer's disease in future studies. Finally, this study does not preclude the possibility that the toxicity from $App^{NL\text{-}G\text{-}F}$ is contributing to the sleep abnormalities. This is another point to be explored in future studies.

4.5 EEG slowing during REMS, consistent with human studies

According to the results of cortical EEG spectral analyses in Alzheimer's disease patients or patients with mild cognitive impairment, alterations in the oscillatory activity during REMS are suggested to be more sensitive biological markers of the disease than

alterations during wake (Petit *et al.*, 1993; Brayet *et al.*, 2016)). In such patients, EEG slowing, i.e., the simultaneous occurrence of an increase in the power of the slow (e.g., delta) component and a decrease in the power of the fast (e.g., alpha or beta) component of the EEG power spectrum during REM sleep was observed. The homozygous mice in our study appeared to well recapitulate the EEG slowing during REMS, which, to our knowledge, is the first report of this in an Alzheimer's disease mouse model. By contrast, some other Alzheimer's disease mouse models exhibit an apparently opposite phenotype, i.e., a decrease in delta or theta power and an increase in gamma power (Zhang *et al.*, 2005; Jyoti *et al.*, 2010; Schneider *et al.*, 2014; Colby-Milley *et al.*, 2015; Kent *et al.*, 2018). Cortical and hippocampal oscillatory activities are regulated by both local circuits and various subcortical areas, including the brainstem.

4.6 Possible mechanism underlying the impaired oscillatory activities

The altered oscillatory activities again highlight the advantage of using a single *App* knock-in mouse, in which the endogenous expression pattern of APP is faithfully recapitulated. For example, ectopic expression or overexpression of APP might lead to impaired inhibitory neurotransmission, considering that secreted APP can act on GABA B receptors (Rice *et al.*, 2019). Of note, in another study utilizing $App^{NL\text{-}G\text{-}F}$ homozygous mice, local field potential measurements with tetrodes from the entorhinal cortex in awake behaving mice detected impaired gamma-theta coupling as early as 5 months (Nakazono *et al.*, 2017). Thus, in future studies, measurements of neural activity during REM sleep with similar devices and analyses may allow for the detection of impaired oscillations at an even earlier age.

4.7 Behavioral impairments in App^{NL-G-F} mice

According to recent studies, App^{NL-G-F} homozygous and heterozygous mice exhibit mild behavioral defects, consistent with the notion that these mice represent a preclinical or early stage of Alzheimer's disease. For example, homozygous mice perform normally in the contextual FC test, a spatial hippocampal-dependent task, even at 15-18 months (Sakakibara *et al.*, 2018). In the current study, using trace FC, which assesses temporal associative memory, we were able to detect a memory deficit in homozygous mice at 7 months. At 13 months, homozygous mice, and to a lesser extent, heterozygous mice exhibited impaired learning.

4.8 Relationship between REMS deficit and learning and memory

Interestingly, at 7 months, there was no correlation between the amount of REMS and learning or memory, whereas at 13 months, there was a strong and positive correlation. Perhaps, the memory deficit and REMS impairment originally develop independently at younger ages, but in the course of disease progression, somehow REMS impairment contributes to worsening of the learning and memory deficit. Post-learning REMS is crucial for memory consolidation (Boyce *et al.*, 2016). As the 13-month-old heterozygous and homozygous mice displayed learning impairments during training, however, it is unlikely that defects of the post-learning sleep are the major cause. Therefore, if the REMS impairment does contribute to learning and memory deficits, it might be that REMS is somehow involved in the daily maintenance of the brain areas related to learning.

4.9 Future direction

Whereas recent studies have begun to elucidate the roles of NREMS in brain maintenance, e.g., by enhancing clearance of metabolites or by downscaling synaptic

excitability (Xie *et al.*, 2013; Norimoto *et al.*, 2018), the contribution of REMS is far less understood. Future studies should address the possibility that impairments in REMS affect brain maintenance and contribute to the progression of Alzheimer's disease.

Bibliography

Anaclet C, Ferrari L, Arrigoni E, Bass CE, Saper CB, Lu J, et al. The GABAergic parafacial zone is a medullary slow wave sleep-promoting center. Nat Neurosci 2014; 17: 1217–24.

de Andrés I, Garzón M, Reinoso-Suárez F. Functional anatomy of non-REM sleep. Front Neurol 2011; NOV: 1–14.

Arruda-Carvalho M, Sakaguchi M, Akers KG, Josselyn SA, Frankland PW. Posttraining Ablation of Adult-Generated Neurons Degrades Previously Acquired Memories. J Neurosci 2011; 31: 15113–27.

Boissard R, Gervasoni D, Schmidt MH, Barbagli B, Fort P, Luppi PH. The rat ponto-medullary network responsible for paradoxical sleep onset and maintenance: A combined microinjection and functional neuroanatomical study. Eur J Neurosci 2002; 16: 1959–73.

Boyce R, Glasgow SD, Williams S, Adamantidis A. Causal evidence for the role of REM sleep theta rhythm in contextual memory consolidation. Science (80-) 2016; 352: 812–16.

Boyce R, Williams S, Adamantidis A. REM sleep and memory. Curr Opin Neurobiol 2017; 44: 167–77.

Brayet P, Petit D, Frauscher B, Gagnon JF, Gosselin N, Gagnon K, et al. Quantitative EEG of Rapid-Eye-Movement Sleep: A Marker of Amnestic Mild Cognitive Impairment. Clin EEG Neurosci 2016; 47: 134–41.

Carpenter BD, Strauss M, Patterson MB. Sleep Disturbances in Community-Dwelling Patients with Alzheimer's disease. Clin Gerontol 1996; 16: 35–49.

Chowdhury N, Quinn JJ, Fanselow MS. Dorsal hippocampus involvement in trace fear conditioning with long, but not short, trace intervals in mice. Behav Neurosci 2005; 119:

1396–402.

Coben LA, Danziger WL, Berg L. Frequency analysis of the resting awake EEG in mild senile dementia of Alzheimer type. Electroencephalogr Clin Neurophysiol 1983; 55: 372–380.

Colby-Milley J, Cavanagh C, Jego S, Breitner JCS, Quirion R, Adamantidis A. Sleep-Wake Cycle Dysfunction in the TgCRND8 Mouse Model of Alzheimer's disease: From Early to Advanced Pathological Stages. PLoS One 2015; 10: e0130177.

DeVos SL, Corjuc BT, Commins C, Dujardin S, Bannon RN, Corjuc D, et al. Tau reduction in the presence of amyloid-β prevents tau pathology and neuronal death in vivo. Brain 2018; 141: 2194–212.

Floyd JA, Janisse JJ, Jenuwine ES, Ager JW. Changes in REM-sleep percentage over the adult lifespan. Sleep 2007; 30: 829–836.

Gais S, Plihal W, Wagner U, Born J. Early sleep triggers memory for early visual discrimination skills. Nat Neurosci 2000; 3: 1335–1339.

Gilmartin MR, Helmstetter FJ. Trace and contextual fear conditioning require neural activity and NMDA receptor-dependent transmission in the medial prefrontal cortex. Learn Mem 2010; 17: 289–96.

Hablitz LM, Vinitsky HS, Sun Q, Stæger FF, Sigurdsson B, Mortensen KN, et al. Increased glymphatic influx is correlated with high EEG delta power and low heart rate in mice under anesthesia. Sci Adv 2019; 5: eaav5447.

Hasselmo ME. The role of acetylcholine in learning and memory. Curr Opin Neurobiol 2006; 16: 710–5.

Hayashi Y, Kashiwagi M, Yasuda K, Ando R, Kanuka M, Sakai K, et al. Cells of a common developmental origin regulate REM/non-REM sleep and wakefulness in mice.

Science (80-) 2015; 350: 957–61.

Herrmann CS, Demiralp T. Human EEG gamma oscillations in neuropsychiatric disorders. Clin Neurophysiol 2005; 116: 2719–33.

Huber R, Felice Ghilardi M, Massimini M, Tononi G. Local sleep and learning. Nature 2004; 430: 78–81.

Huerta PT, Sun LD, Wilson MA, Tonegawa S. Formation of temporal memory requires NMDA receptors within CA1 pyramidal neurons. Neuron 2000; 25: 473–80.

Ju YES, McLeland JS, Toedebusch CD, Xiong C, Fagan AM, Duntley SP, et al. Sleep quality and preclinical Alzheimer disease. JAMA Neurol 2013; 70: 587–93.

Jyoti A, Plano A, Riedel G, Platt B. EEG, Activity, and Sleep Architecture in a Transgenic AβPPswe/PSEN1A246E Alzheimer's disease Mouse. J Alzheimer's Dis 2010; 22: 873–87.

Kang J-E, Lim MM, Bateman RJ, Lee JJ, Smyth LP, Cirrito JR, et al. Amyloid-beta Dynamics Are Regulated by Orexin and the Sleep-Wake Cycle. Science (80-) 2009; 326: 1005–7.

Karni A, Tanne D, Rubenstein B, Askenasy J, Sagi D. Dependence on REM sleep of overnight improvement of a perceptual skill. Science (80-) 1994; 265: 679–82.

Kent BA, Strittmatter SM, Nygaard HB. Sleep and EEG Power Spectral Analysis in Three Transgenic Mouse Models of Alzheimer's disease: APP/PS1, 3xTgAD, and Tg2576. J Alzheimer's Dis 2018; 64: 1325–36.

Koenig T, Prichep L, Dierks T, Hubl D, Wahlund LO, John ER, et al. Decreased EEG synchronization in Alzheimer's disease and mild cognitive impairment. Neurobiol Aging 2005; 26: 165–71.

Lee MG, Hassani OK, Alonso A, Jones BE. Cholinergic basal forebrain neurons burst

with theta during waking and paradoxical sleep. J Neurosci 2005; 25: 4365–9.

Liguori C, Romigi A, Nuccetelli M, Zannino S, Sancesario G, Martorana A, et al. Orexinergic system dysregulation, sleep impairment, and cognitive decline in Alzheimer disease. JAMA Neurol 2014; 71: 1498–505.

Lu J, Sherman D, Devor M, Saper CB. A putative flip–flop switch for control of REM sleep. Nature 2006; 441: 589–94.

Lucey BP, McCullough A, Landsness EC, Toedebusch CD, McLeland JS, Zaza AM, et al. Reduced non–rapid eye movement sleep is associated with tau pathology in early Alzheimer's disease. Sci Transl Med 2019; 11: eaau6550.

Malhotra RK. Neurodegenerative Disorders and Sleep. Sleep Med Clin 2018; 13: 63–70.

Marks GA, Shaffery JP, Oksenberg A, Speciale SG, Roffwarg HP. A functional role for REM sleep in brain maturation. Behav Brain Res 1995; 69: 1–11.

McCurry SM, Logsdon RG, Teri L, Gibbons LE, Kukull WA, Bowen JD, et al. Characteristics of Sleep Disturbance in Community-Dwelling Alzheimer's disease Patients. J Geriatr Psychiatry Neurol 1999; 12: 53–59.

McEchron MD, Bouwmeester H, Tseng W, Weiss C, Disterhoft JF. Hippocampectomy disrupts auditory trace fear conditioning and contextual fear conditioning in the rat. Hippocampus 1998; 8: 638–46.

Minakawa EN, Miyazaki K, Maruo K, Yagihara H, Fujita H, Wada K, et al. Chronic sleep fragmentation exacerbates amyloid β deposition in Alzheimer's disease model mice. Neurosci Lett 2017; 653: 362–69.

Misane I, Tovote P, Meyer M, Spiess J, Ögren SO, Stiedl O. Time-dependent involvement of the dorsal hippocampus in trace fear conditioning in mice. Hippocampus 2005; 15: 418–26.

Moran M, Lynch CA, Walsh C, Coen R, Coakley D, Lawlor BA. Sleep disturbance in mild to moderate Alzheimer's disease. Sleep Med 2005; 6: 347–52.

Nakazono T, Lam TN, Patel AY, Kitazawa M, Saito T, Saido TC, et al. Impaired In Vivo Gamma Oscillations in the Medial Entorhinal Cortex of Knock-in Alzheimer Model. Front Syst Neurosci 2017; 11: 1–12.

Norimoto H, Makino K, Gao M, Shikano Y, Okamoto K, Ishikawa T, et al. Hippocampal ripples down-regulate synapses - supplementary info. Science (80-) 2018; 1527: 1–8.

Ozen Irmak S, de Lecea L. Basal Forebrain Cholinergic Modulation of Sleep Transitions. Sleep 2014; 37: 1941–1951.

Pase MP, Himali JJ, Grima NA, Beiser AS, Satizabal CL, Aparicio HJ, et al. Sleep architecture and the risk of incident dementia in the community. Neurology 2017; 89: 1244–50.

Petit D, Lorrain D, Gauthier S, Montplaisir J. Regional spectral analysis of the REM sleep EEG in mild to moderate Alzheimer's disease. Neurobiol Aging 1993; 14: 141–5.

Platt B, Drever B, Koss D, Stoppelkamp S, Jyoti A, Plano A, et al. Abnormal cognition, sleep, eeg and brain metabolism in a novel knock-in alzheimer mouse, plb1. PLoS One 2011; 6

Prinz PN, Larsen LH, Moe KE, Vitiello M V. EEG markers of early Alzheimer's disease in computer selected tonic REM sleep. Electroencephalogr Clin Neurophysiol 1992; 83: 36–43.

Prinz PN, Vitaliano PP, Vitiello M V., Bokan J, Raskind M, Peskind E, et al. Sleep, EEG and mental function changes in senile dementia of the Alzheimer's type. Neurobiol Aging 1982; 3: 361–70.

Purple RJ, Sakurai T, Sakaguchi M. Auditory conditioned stimulus presentation during

NREM sleep impairs fear memory in mice. Sci Rep 2017; 7: 46247.

Quinn JJ, Oommen SS, Morrison GE, Fanselow MS. Post-training excitotoxic lesions of the dorsal hippocampus attenuate forward trace, backward trace, and delay fear conditioning in a temporally specific manner. Hippocampus 2002; 12: 495–504.

Rice HC, de Malmazet D, Schreurs A, Frere S, Van Molle I, Volkov AN, et al. Secreted amyloid-β precursor protein functions as a GABA B R1a ligand to modulate synaptic transmission. Science (80-) 2019; 363: eaao4827.

Rod NH, Vahtera J, Westerlund H, Kivimaki M, Zins M, Goldberg M, et al. Sleep disturbances and cause-specific mortality: Results from the GAZEL cohort study. Am J Epidemiol 2011; 173: 300–309.

Roh JH, Huang Y, Bero AW, Kasten T, Stewart FR, Bateman RJ, et al. Disruption of the sleep-wake cycle and diurnal fluctuation of beta-amyloid in mice with Alzheimer's disease pathology. Sci Transl Med 2012; 4: 150ra122.

Saito T, Matsuba Y, Mihira N, Takano J, Nilsson P, Itohara S, et al. Single App knock-in mouse models of Alzheimer's disease. Nat Neurosci 2014; 17: 661–3.

Sakai K, Crochet S, Onoe H. Pontine structures and mechanisms involved in the generation of paradoxical (REM) sleep. Arch Ital Biol 2001; 139: 93–107.

Sakakibara Y, Sekiya M, Saito T, Saido TC, Iijima KM. Cognitive and emotional alterations in App knock-in mouse models of Aβ amyloidosis. BMC Neurosci 2018; 19: 46.

Sasaguri H, Nilsson P, Hashimoto S, Nagata K, Saito T, De Strooper B, et al. APP mouse models for Alzheimer's disease preclinical studies. EMBO J 2017; 36: 2473–87.

Schiffelholz T, Aldenhoff JB. Novel object presentation affects sleep-wake behavior in rats. Neurosci Lett 2002; 328: 41–4.

Schneider F, Baldauf K, Wetzel W, Reymann KG. Behavioral and EEG changes in male 5xFAD mice. Physiol Behav 2014; 135: 25–33.

Seibenhener ML, Wooten MC. Use of the Open Field Maze to Measure Locomotor and Anxiety-like Behavior in Mice. J Vis Exp 2015: e52434.

Sethi M, Joshi SS, Webb RL, Beckett TL, Donohue KD, Murphy MP, et al. Increased fragmentation of sleep–wake cycles in the 5XFAD mouse model of Alzheimer's disease. Neuroscience 2015; 290: 80–9.

Shokri-Kojori E, Wang G-J, Wiers CE, Demiral SB, Guo M, Kim SW, et al. β-Amyloid accumulation in the human brain after one night of sleep deprivation. Proc Natl Acad Sci U S A 2018; 115: 4483–8.

Vazquez J, Baghdoyan HA. Basal forebrain acetylcholine release during REM sleep is significantly greater than during waking. Am J Physiol Integr Comp Physiol 2001; 280: R598–R601.

Weber F, Chung S, Beier KT, Xu M, Luo L, Dan Y. Control of REM sleep by ventral medulla GABAergic neurons. Nature 2015; 526: 435–8.

Westerberg CE, Mander BA, Florczak SM, Weintraub S, Mesulam M-M, Zee PC, et al. Concurrent Impairments in Sleep and Memory in Amnestic Mild Cognitive Impairment. J Int Neuropsychol Soc 2012; 18: 490–500.

Whitehouse P, Price D, Struble R, Clark A, Coyle J, Delon M. Alzheimer's disease and senile dementia: loss of neurons in the basal forebrain. Science (80-) 1982; 215: 1237–9.

Whitehouse PJ, Price DL, Clark AW, Coyle JT, DeLong MR. Alzheimer disease: evidence for selective loss of cholinergic neurons in the nucleus basalis. Ann Neurol 1981; 10: 122–6.

Whyte LS, Hemsley KM, Lau AA, Hassiotis S, Saito T, Saido TC, et al. Reduction in open field activity in the absence of memory deficits in the AppNL−G−Fknock-in mouse model of Alzheimer's disease. Behav Brain Res 2018; 336: 177–81.

Xie L, Kang H, Xu Q, Chen MJ, Liao Y, Thiyagarajan M, et al. Sleep Drives Metabolite Clearance from the Adult Brain. Science (80-) 2013; 342: 373–7.

Xu M, Chung S, Zhang S, Zhong P, Ma C, Chang WC, et al. Basal forebrain circuit for sleep-wake control. Nat Neurosci 2015; 18: 1641–7.

Yoder RM, Pang KCH. Involvement of GABAergic and cholinergic medial septal neurons in hippocampal theta rhythm. Hippocampus 2005; 15: 381–92.

Zhang B, Veasey SC, Wood MA, Leng LZ, Kaminski C, Leight S, et al. Impaired Rapid Eye Movement Sleep in the Tg2576 APP Murine Model of Alzheimer's disease with Injury to Pedunculopontine Cholinergic Neurons. Am J Pathol 2005; 167: 1361–9.

Zhang J, Paksarian D, Lamers F, Hickie IB, He J, Merikangas KR. Sleep Patterns and Mental Health Correlates in US Adolescents. J Pediatr 2017; 182: 137–143.

Zhou J, Zhang J, Lam SP, Tang X, Wing YK. Clinical Biomarkers of Neurodegeneration in REM Sleep Behavior Disorder. J Sleep Med 2015; 12: 27–33.

Zhu H, Yan H, Tang N, Li X, Pang P, Li H, et al. Impairments of spatial memory in an Alzheimer's disease model via degeneration of hippocampal cholinergic synapses. Nat Commun 2017; 8: 1676.

Supplementary Figures

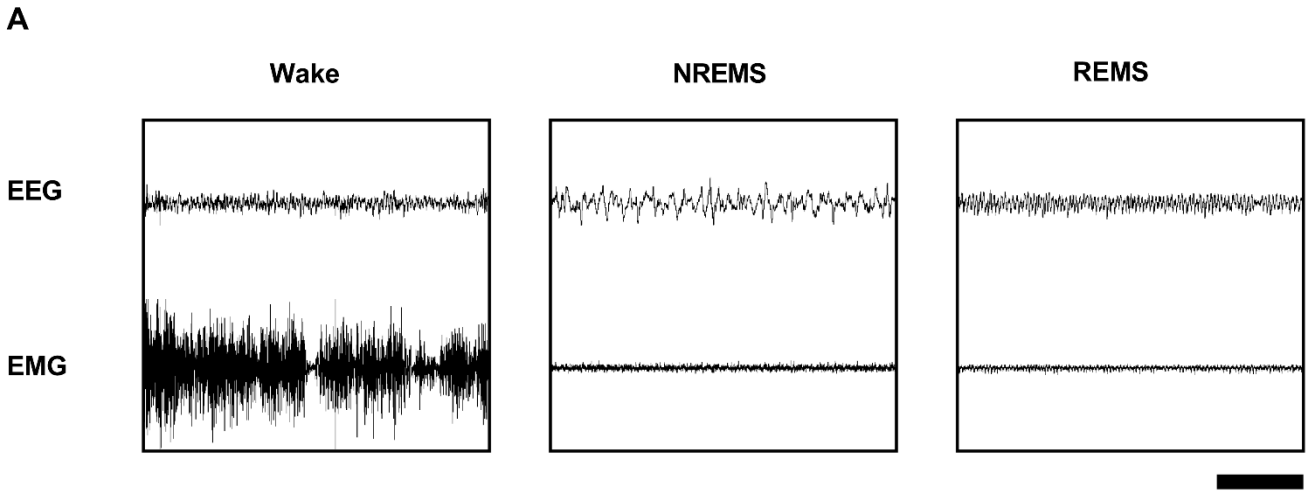

Supplementary figure 1. Representative images of EEG/EMG signals.

Scale bar: 3 s.

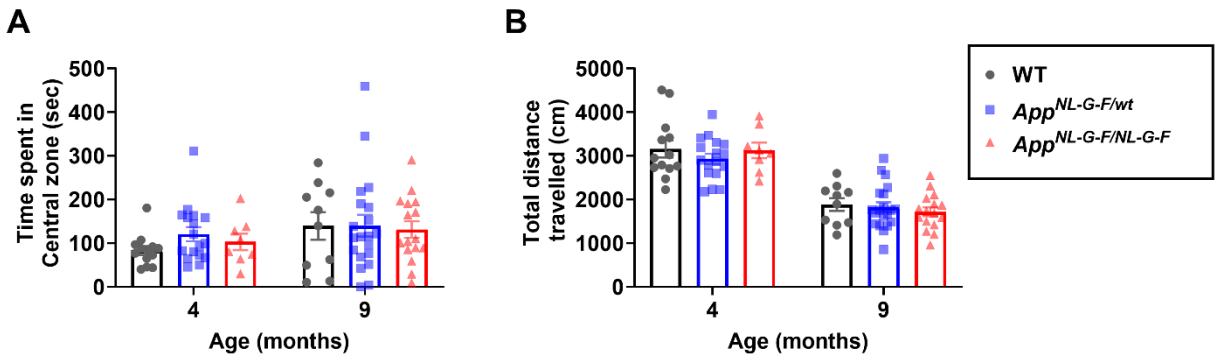

Supplementary figure 2. Normal performance in the OFT in *App*$^{NL-G-F}$ mice.

(A and B) Time spent in the central zone **[A]** and total distance travelled **[B]** by 4-month-old and 9-month-old mice. Bar graphs represent mean ± SEM. Each point represents an individual mouse. Detailed results of the statistical tests are described in Supplementary Table 6.

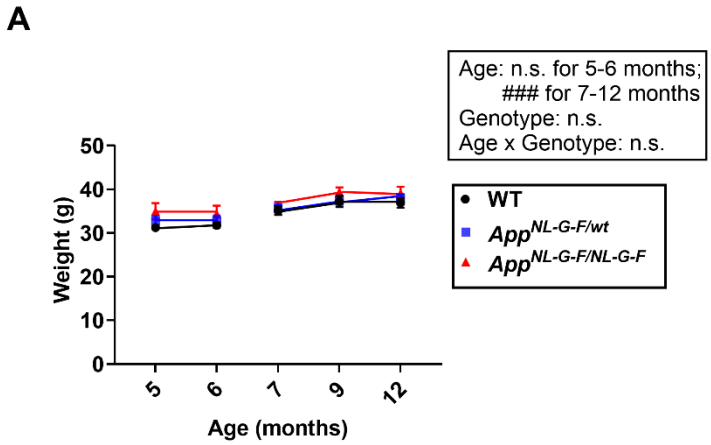

Supplementary figure 3. Normal body weight in *App*$^{NL\text{-}G\text{-}F}$ mice.

Each point represents mean ± SEM. The body weight of the younger mice was measured at 5 and 6 months while the body weight of the older mice was measured at 7, 9, and 12 months. Each point represents the mean ± SEM. Detailed results of the statistical tests are described in Supplementary Table 7.

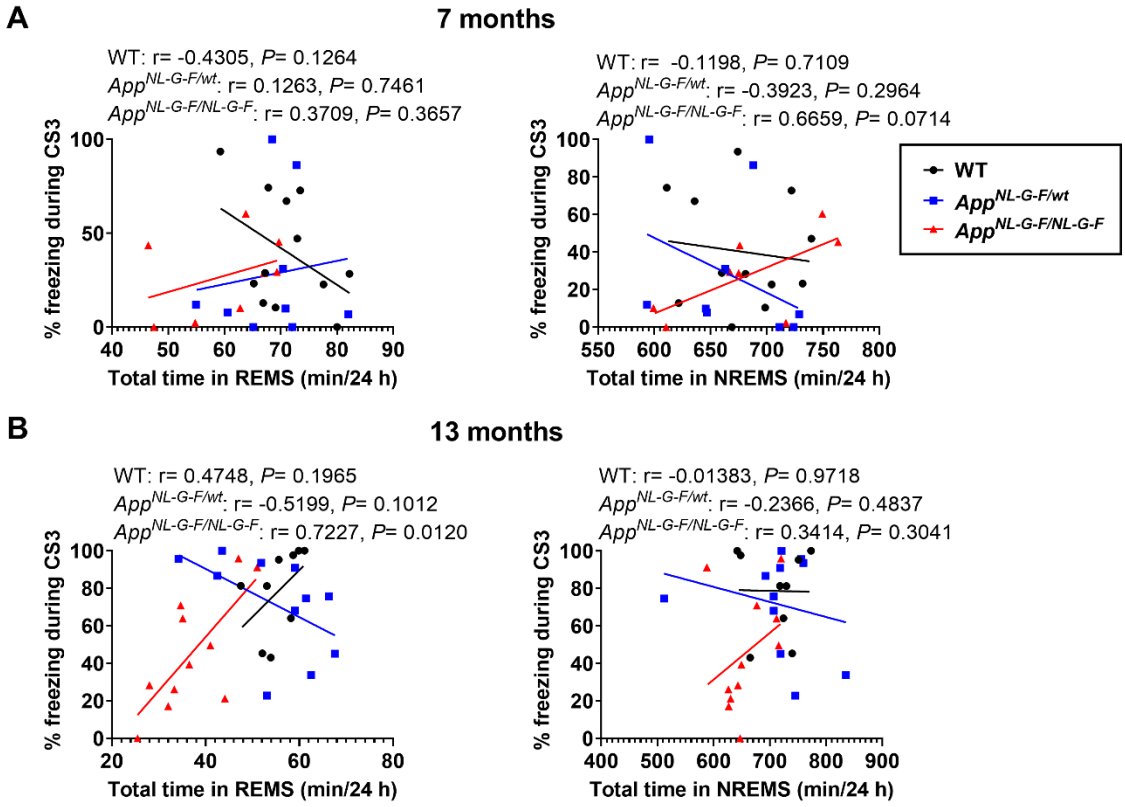

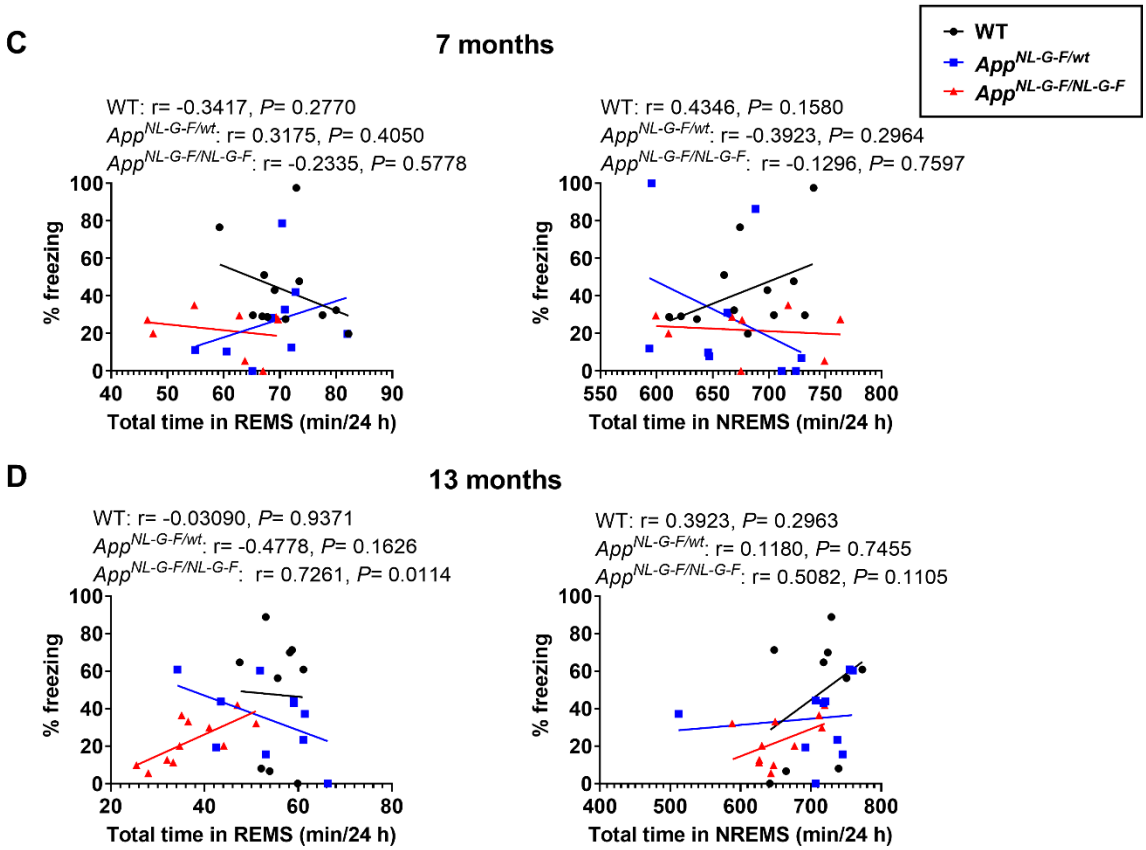

Supplementary figure 4. Correlations between the amount of time spent in each sleep stage and freezing rate in trace FC. (A-D) Correlation between total amount of REMS or NREMS and percent time spent freezing during the third CS on day 1 (training) **[A, B]** or the CS on day 2 (retrieval) **[C-D]** in younger **[A, C]** or older **[B, D]** mice. Each point represents an individual mouse. The Pearson's correlation coefficient (r) and *P* value are provided for each genotype.

Supplementary Tables

Supplementary table 1. Detailed results of the statistical analyses in Figure 1.

Figure number	Sample size (n)	Mixed ANOVA	Games-Howell
1A (Wake)	WT: n= 12 mice; *App* $^{NL\text{-}G\text{-}F/wt}$: n= 11 mice; *App* $^{NL\text{-}G\text{-}F/NL\text{-}G\text{-}F}$: n= 8 mice	time: F(11,308)= 105.702, P=0.000 time*genotype: F(22,308)= 1.068, P=0.381 genotype: F(2,28)= 0.540, P=0.589	n.a.
1A (NREMS)		time: F(11,308)= 93.267, P=0.000 time*genotype: F(22,308) = 0.966, P=0.508 genotype: F(2,28)= 0.748, P=0.483	n.a.
1A (REMS)		time: F(11,308)= 99.036, P=0.000 time*genotype: F(22,308)= 1.669, P=0.032 genotype: F(2,28)=5.040, P=0.014	WT vs *App* $^{NL\text{-}G\text{-}F/wt}$: ZT 2: t(20.921)=0.195, *P*=0.979, 95% CI: -1.547, 1.808, ZT 4: t(17.299)=0.758, *P*=0.733 , 95% CI: -2.188, 1.189, ZT 6: t(19.962)=1.369, *P*=0.375, 95% CI: -0.568, 1.907, ZT 8: t(16.122)=1.357, *P*=0.385, 95% CI: -1.659, 0.514, ZT 10: t(19.771)=0.455, *P*=0.893, 95% CI: -0.812, 1.168, ZT 12: t(19.623)=0.210, *P*=0.976, 95% CI: -0.989, 1.168, ZT 14: t(18.352)=1.150, *P*=0.497, 95% CI: -0.223, 0.590, ZT 16: t(18.242)=1.393, *P*= 0.365, 95% CI: -1.111, 0.326, ZT 18: t(13.045)=3.298, *P*=0.015, 95% CI: -1.750, -0.194ZT 20: t(17.429)=1.333, *P*= 0.396, 95% CI: -0.374, 0.188, ZT 22: t(20.209)=0.268, *P*=0.961, 95% CI: -1.478, 1.194, ZT 24: t(18.681)=0.496, *P*= 0.874, 95% CI: -1.456, 0.980

1A (REMS)	WT: n= 12 mice; *App* $^{NL\text{-}G\text{-}F/wt}$: n= 11 mice; *App* $^{NL\text{-}G\text{-}F/NL\text{-}G\text{-}F}$: n= 8 mice	time: F(11,308)= 99.036, P=0.000 time*genotype: F(22,308)= 1.669, P=0.032 genotype: F(2,28)=5.040, P=0.014	WT vs *App* $^{NL\text{-}G\text{-}F/NL\text{-}G\text{-}F}$: ZT 2: t(16.939)=1.372, *P*=0.377, 95% CI: -2.790, 0.846, ZT 4: t(17.698)=3.930, *P*=0.003 , 95% CI: -3.127, -0.662, ZT 6: t(13.373)=1.047, *P*=0.561, 95% CI: -1.972, 0.847, ZT 8: t(14.528)=1.257, *P*=0.440, 95% CI: -1.579, 0.551, ZT 10: t(14.814)=1.308, *P*=0.413, 95% CI: -1.984, 0.656, ZT 12: t(16.958)=1.457, *P*=0.336, 95% CI: -1.530, 0.422, ZT 14: t(17.689)=0.256, *P*=0.965, 95% CI: -0.351, 0.287, ZT 16: t(13.415)=0.219, *P*= 0.974, 95% CI: -1.191, 1.008, ZT 18: t(17.768)=0.672, *P*=0.782, 95% CI: -1.220, 0.712, ZT 20: t(8.262)=1.525, *P*= 0.329, 95% CI: -0.764, 2.539, ZT 22: t(15.403)=1.636, *P*=0.261, 95% CI: -2.272, 0.513, ZT 24: t(11.794)=0.160, *P*= 0.986, 95% CI: -1.399, 1.577
			App $^{NL\text{-}G\text{-}F/wt}$ vs *App* $^{NL\text{-}G\text{-}F/NL\text{-}G\text{-}F}$: ZT 2: t(15.493)=1.637, *P*=0.261, 95% CI: -2.846, 0.641, ZT 4: t(15.434)=2.172, *P*=0.108 , 95% CI: -3.058, 0.269, ZT 6: t(15.321)=2.139, *P*=0.115, 95% CI: -2.725, 0.261, ZT 8: t(17.000)=0.236, *P*=0.970, 95% CI: -0.575, 0.692, ZT 10: t(11.623)=1.827, *P*=0.204, 95% CI: -2.076, 0.393, ZT 12: t(16.992)=1.500, *P*=0.316, 95% CI: -1.744, 0.457, ZT 14: t(16.079)=1.391, *P*=0.369, 95% CI: -0.615 ,0.184, ZT 16: t(9.670)=0.803, *P*= 0.710, 95% CI: -0.731, 1.333, ZT 18: t(8.662)=2.694, *P*=0.060, 95% CI: -0.032, 1.467, ZT 20: t(9.945)=0.784, *P*= 0.721, 95% CI: -1.202, 2.164, ZT 22: t(16.290)=1.282, *P*=0.425, 95%

1A (REMS)	WT: WT: n= 12 mice; *App* $^{NL\text{-}G\text{-}F/wt}$: n= 11 mice; *App* $^{NL\text{-}G\text{-}F/NL\text{-}G\text{-}F}$: n= 8 mice		CI: -2.219, 0.744, ZT 24: t(14.708)=0.530, *P*= 0.858, 95% CI: -1.277, 1.930
1B (Wake)		time: F(11,352)= 86.674, P=0.000 Time*genotype: F (22,352) = 1.401, P=0.110 genotype: F (2, 32) =4.591. P=0.018 P=0.018	n.a.
1B (NREMS)		time: F(11,352)= 77.379, P=0.000 time*genotype: F(22,352)= 1.521, P=0.064 genotype: F(2,32)=2.637, P=0.087	n.a.
1B (REMS)	WT: n= 10 mice; *App* $^{NL\text{-}G\text{-}F/wt}$: n= 12 mice; *App* $^{NL\text{-}G\text{-}F/NL\text{-}G\text{-}F}$: n= 13 mice	time: F(11,352)= 103.011, P=0.000 time*genotype: F(22,352)= 2.720, P=0.000 genotype: F(2,32)=20.638, P=0.000	WT vs *App* $^{NL\text{-}G\text{-}F/wt}$: ZT 2: t(19.924)=1.604, *P*=0.267, 95% CI: -1.720, 0.386, ZT 4: t(17.755)=0.745, *P*=0.741 , 95% CI: -0.920, 1.676, ZT 6: t(18.881)=0.440, *P*=0.900, 95% CI: -1.556, 1.907, ZT 8: t(19.393)=1.099, *P*=0.526, 95% CI: -1.520, 0.601, ZT 10: t(18.113)=1.110, *P*=0.520, 95% CI: -1.713, 0.675, ZT 12: t(19.987)=0.994, *P*=0.589, 95% CI: -0.511, 1.174, ZT 14: t(16.331)=0.636, *P*=0.803, 95% CI: -0.429, 0.710, ZT 16: t(15.966)=1.634, *P*= 0.261, 95% CI: -0.261, 1.161, ZT 18: (18.463)=0.175, *P*=0.983, 95% CI: -0.899, 0.784, ZT 20: t(18.265)=1.476, *P*= 0.325, 95% CI: -0.402, 1.507, ZT 22: t(19.863)=0.132, *P*=0.990, 95% CI: -1.565, 1.409, ZT 24: t(19.918)=0.522, *P*= 0.861, 95% CI: -0.716, 1.088

1B (REMS)	WT: n= 10 mice; *App* $^{NL\text{-}G\text{-}F/wt}$: n= 12 mice; *App* $^{NL\text{-}G\text{-}F/NL\text{-}G\text{-}F}$: n= 13 mice	time: F(11,352)= 103.011, P=0.000 time*genotype: F(22,352)= 2.720, P=0.000 genotype: F(2,32)=20.638, P=0.000	WT vs *App* $^{NL\text{-}G\text{-}F/NL\text{-}G\text{-}F}$: ZT 2: t(19.926)=4.720, *P*=0.000, 95% CI: -2.837, -0.857, ZT 4: t(14.079)=4.027, *P*=0.003, 95% CI: -3.033, -0.645, ZT 6: t(18.721)=2.769, *P*=0.032, 95% CI: -2.703, -0.115, ZT 8: t(17.999)=2.975, *P*=0.021, 95% CI: -2.135, -0.163, ZT 10: t(14.753)=2.669, *P*=0.044, 95% CI: -2.225, -0.028, ZT 12: t(20.986)=2.276, *P*=0.082, 95% CI: -1.590, 0.08, ZT 14:t(20.811)=0.231, *P*=0.971, 95% CI: -0.380, 0.456, ZT 16: t(20.292)=0.518, *P*= 0.863, 95% CI: -0.343, 0.520, ZT 18: t(17.969)=0.010, *P*=1.000, 95% CI: -0.841, 0.821, ZT 20: t(20.958)=0.177, *P*= 0.983, 95% CI: -0.712, 0.820, ZT 22: t(14.577)=1.758, *P*=0.218, 95% CI: -2.065, 0.401, ZT 24: t(12.903)=0.775, *P*= 0.724, 95% CI: -0.933, 0.510
			App $^{NL\text{-}G\text{-}F/wt}$ vs *App* $^{NL\text{-}G\text{-}F/NL\text{-}G\text{-}F}$: ZT 2: t(22.364)=2.952, *P*=0.019, 95% CI: -2.183, -0.177, ZT 4: t(19.971)=5.862, *P*=0.000 , 95% CI: -3.174, -1.260 E13, ZT 6: t(22.746)=2.514, *P*=0.049, 95% CI: -2.355, -0.004, ZT 8: t(21.819)=1.871, *P*=0.171, 95% CI: -1.616, 0.237, ZT 10: t(20.377)=1.686, *P*=0.234, 95% CI: -1.518, 0.303, ZT 12: t(22.939)=3.085, *P*=0.014, 95% CI: -1.967, -0.204, ZT 14: t(19.399)=0.435, *P*=0.902, 95% CI: -0.699 ,0.495, ZT 16: t(15.867)=1.323, *P*= 0.403, 95% CI: -1.067, 0.344, ZT 18: t(22.651)=0.213, *P*=0.975, 95% CI: -0.657, 0.780, ZT 20: t(20.295)=1.291, *P*= 0.416, 95% CI: -1.982, 0.474, ZT 22:

1B (REMS)			t(17.649)=1.573, *P*=0.283, 95% CI: -1.982, 0.474, ZT 24: t(15.347)=1.414, *P*= 0.359, 95% CI: -1.127, 0.331
1C (Wake)	6-month-old mice: WT: n= 12 mice; *App* $^{NL\text{-}G\text{-}F/wt}$: n= 11 mice; *App* $^{NL\text{-}G\text{-}F/NL\text{-}G\text{-}F}$: n= 8 mice; 12-month-old mice: WT: n= 10 mice; *App* $^{NL\text{-}G\text{-}F/wt}$: n= 12 mice; *App* $^{NL\text{-}G\text{-}F/NL\text{-}G\text{-}F}$: n= 13 mice	n.a.	6 months: WT vs *App* $^{NL\text{-}G\text{-}F/wt}$: t(19.329)=1.142, *P*=0.501, 95% CI: -28.961, 76.372 WT vs *App* $^{NL\text{-}G\text{-}F/NL\text{-}G\text{-}F}$: t(11.451)=0.301, *P*=0.951, 95% CI: -61.347, 76.836 *App* $^{NL\text{-}G\text{-}F/wt}$ vs *App* $^{NL\text{-}G\text{-}F/NL\text{-}G\text{-}F}$: t(13.775)=0.574, *P*=0.836, 95% CI: -88.800, 56.883 12 months: WT vs *App* $^{NL\text{-}G\text{-}F/wt}$: t(18.638)=0.433, *P*=0.902, 95% CI: -76.865, 54.509 WT vs App $^{NL\text{-}G\text{-}F/NL\text{-}G\text{-}F}$: t(19.493)=3.478, *P*=0.007, 95% CI: 18.169, 115.882 *App* $^{NL\text{-}G\text{-}F/wt}$ vs *App* $^{NL\text{-}G\text{-}F/NL\text{-}G\text{-}F}$: t(18.076)=3.148, *P*=0.015, 95% CI:14.819, 141.588
1C (NREMS)		n.a.	6 months: WT vs *App* $^{NL\text{-}G\text{-}F/wt}$: t(19.728)=1.106, *P*=0.521, 95% CI: -70.350, 27.573 WT vs *App* $^{NL\text{-}G\text{-}F/NL\text{-}G\text{-}F}$: t(11.674)=0.129, *P*=0.991, 95% CI: -61.811, 68.083 *App* $^{NL\text{-}G\text{-}F/wt}$ vs *App* $^{NL\text{-}G\text{-}F/NL\text{-}G\text{-}F}$: t(13.525)=0.951, *P*=0.619, 95% CI: -43.249,92.299 12 months: WT vs *App* $^{NL\text{-}G\text{-}F/wt}$: t(18.523)=0.416, *P*=0.909, 95% CI: -55.238, 76.831 WT vs *App* $^{NL\text{-}G\text{-}F/NL\text{-}G\text{-}F}$: t(19.301)=2.596, *P*=0.044, 95% CI: -97.640, -1.113 *App* $^{NL\text{-}G\text{-}F/wt}$ vs *App* $^{NL\text{-}G\text{-}F/NL\text{-}G\text{-}F}$: t(17.704)=2.420, *P*=0.065, 95% CI:-123.721, 3.375

1C (REMS)	6-month-old mice: WT : n= 12 mice; *App* $^{NL\text{-}G\text{-}F/wt}$: n= 11 mice; *App* $^{NL\text{-}G\text{-}F/NL\text{-}G\text{-}F}$: n= 8 mice; 12-month-old mice: WT: n= 10 mice; *App* $^{NL\text{-}G\text{-}F/wt}$: n= 12 mice; *App* $^{NL\text{-}G\text{-}F/NL\text{-}G\text{-}F}$: n= 13 mice	n.a.	6 months: WT vs *App* $^{NL\text{-}G\text{-}F/wt}$: t(20.008)=0.783, *P*=0.717, 95% CI: -9.801, 5.167 WT vs *App* $^{NL\text{-}G\text{-}F/NL\text{-}G\text{-}F}$: t(11.537)=2.842, *P*=0.038, 95% CI: -21.154, -0.612 *App* $^{NL\text{-}G\text{-}F/wt}$ vs *App* $^{NL\text{-}G\text{-}F/NL\text{-}G\text{-}F}$: t(13.050)=2.129, *P*=0.112, 95% CI: -19.187,2.053 12 months: WT vs *App* $^{NL\text{-}G\text{-}F/wt}$: t(15.980)=0.112, *P*=0.993, 95% CI: -8.277, 9.028 WT vs *App* $^{NL\text{-}G\text{-}F/NL\text{-}G\text{-}F}$: t(20.574)=7.082, *P*=0.000, 95% CI: -23.989, -11.310 *App* $^{NL\text{-}G\text{-}F/wt}$ vs *App* $^{NL\text{-}G\text{-}F/NL\text{-}G\text{-}F}$: t(19.518)=4.991, *P*=0.000, 95% CI:-27.179, -8.871
1C (REMS/Total sleep ratio)		n.a.	6 months: WT vs *App* $^{NL\text{-}G\text{-}F/wt}$: t(20.997)=0.068, *P*=0.997, 95% CI: -0.009, 0.008 WT vs *App* $^{NL\text{-}G\text{-}F/NL\text{-}G\text{-}F}$: t(12.170)=2.891, *P*=0.033, 95% CI: -0.026, -0.001 *App* $^{NL\text{-}G\text{-}F/wt}$ vs *App* $^{NL\text{-}G\text{-}F/NL\text{-}G\text{-}F}$: t(11.557)=2.886, *P*=0.035, 95% CI: -0.026, -0.001 12 months: WT vs *App* $^{NL\text{-}G\text{-}F/wt}$: t(15.934)=0.003, *P*=1.000, 95% CI: -0.014,0.014 WT vs *App* $^{NL\text{-}G\text{-}F/NL\text{-}G\text{-}F}$: t(20.879)=4.877, *P*=0.000, 95% CI: -0.028, -0.009 *App* $^{NL\text{-}G\text{-}F/wt}$ vs *App* $^{NL\text{-}G\text{-}F/NL\text{-}G\text{-}F}$: t(18.599)=3.301, *P*=0.010, 95% CI:-0.033, -0.004

1D (Wake)	6-month-old mice: WT: n= 12 mice; *App* $^{NL\text{-}G\text{-}F/wt}$: n= 11 mice; *App* $^{NL\text{-}G\text{-}F/NL\text{-}G\text{-}F}$: n= 8 mice; 12-month-old mice: WT: n= 10 mice; *App* $^{NL\text{-}G\text{-}F/wt}$: n= 12 mice; *App* $^{NL\text{-}G\text{-}F/NL\text{-}G\text{-}F}$: n= 13 mice	n.a.	6 months: WT vs *App* $^{NL\text{-}G\text{-}F/wt}$: t(20.859)=1.491, *P*=0.315, 95% CI: -32.670, 8.391 WT vs *App* $^{NL\text{-}G\text{-}F/NL\text{-}G\text{-}F}$: t(15.572)=0.859, *P*=0.673, 95% CI: -32.593, 16.343 *App* $^{NL\text{-}G\text{-}F/wt}$ vs App $^{NL\text{-}G\text{-}F/NL\text{-}G\text{-}F}$: t(13.922)=0.446, *P*=0.897, 95% CI: -19.532, 27.561 12 months: WT vs *App* $^{NL\text{-}G\text{-}F/wt}$: t(19.886)=0.424, *P*=0.906, 95% CI: -22.280,31.253 WT vs *App* $^{NL\text{-}G\text{-}F/NL\text{-}G\text{-}F}$: t(20.962)=2.292, *P*=0.079, 95% CI: -2.430,51.198 *App* $^{NL\text{-}G\text{-}F/wt}$ vs *App* $^{NL\text{-}G\text{-}F/NL\text{-}G\text{-}F}$: t(22.974)=1.727, *P*=0.217, 95% CI:-8.957, 48.752
1D (NREMS)		n.a.	6 months: WT vs *App* $^{NL\text{-}G\text{-}F/wt}$: t(20.995)=1.567, *P*=0.282, 95% CI: -7.397, 31.696 WT vs *App* $^{NL\text{-}G\text{-}F/NL\text{-}G\text{-}F}$: t(14.567)=2.026, *P*=0.141, 95% CI: -5.279, 42.173 *App* $^{NL\text{-}G\text{-}F/wt}$ vs *App* $^{NL\text{-}G\text{-}F/NL\text{-}G\text{-}F}$: t(13.976)=0.700, *P*=0.767, 95% CI: -17.255, 29.851 12 months: WT vs *App* $^{NL\text{-}G\text{-}F/wt}$: t(18.985)=0.221, *P*=0.973, 95% CI: -28.983,24.343 WT vs *App* $^{NL\text{-}G\text{-}F/NL\text{-}G\text{-}F}$: t(20.709)=0.831, *P*=0.689, 95% CI: -33.492,16.903 *App* $^{NL\text{-}G\text{-}F/wt}$ vs *App* $^{NL\text{-}G\text{-}F/NL\text{-}G\text{-}F}$: t(22.673)=0.512, *P*=0.866, 95% CI:-35.217, 23.268

1D (REMS)	6-month-old mice: WT: n= 12 mice; *App* $^{NL\text{-}G\text{-}F/wt}$: n= 11 mice; *App* $^{NL\text{-}G\text{-}F/NL\text{-}G\text{-}F}$: n= 8 mice; 12-month-old mice: WT: n= 10 mice; *App* $^{NL\text{-}G\text{-}F/wt}$: n= 12 mice; *App* $^{NL\text{-}G\text{-}F/NL\text{-}G\text{-}F}$: n= 13 mice	n.a.	6 months: WT vs *App* $^{NL\text{-}G\text{-}F/wt}$: t(20.507)=0.004, *P*=1.000, 95% CI: -6.434, 6.414 WT vs *App* $^{NL\text{-}G\text{-}F/NL\text{-}G\text{-}F}$: t(17.940)=3.995, *P*=0.002, 95% CI: -16.918, -3.726 *App* $^{NL\text{-}G\text{-}F/wt}$ vs *App* $^{NL\text{-}G\text{-}F/NL\text{-}G\text{-}F}$: t(16.231)=4.452, *P*=0.001, 95% CI: -16.280, -4.344 12 months: WT vs *App* $^{NL\text{-}G\text{-}F/wt}$: t(19.905)=0.788, *P*=0.714, 95% CI: -9.147,4.802 WT vs *App* $^{NL\text{-}G\text{-}F/NL\text{-}G\text{-}F}$: t(20.300)=6.534, *P*=0.000, 95% CI: -22.313,-9.867 *App* $^{NL\text{-}G\text{-}F/wt}$ vs *App* $^{NL\text{-}G\text{-}F/NL\text{-}G\text{-}F}$: t(21.626)=5.135, *P*=0.000, 95% CI:-20.734, -7.101
1D (REMS/Total sleep ratio)		n.a.	6 months: WT vs *App* $^{NL\text{-}G\text{-}F/wt}$: t(20.950)=0.560, *P*=0.843, 95% CI: -0.015, 0.010 WT vs *App* $^{NL\text{-}G\text{-}F/NL\text{-}G\text{-}F}$: t(17.493)=4.502, *P*=0.001, 95% CI: -0.035, -0.010 *App* $^{NL\text{-}G\text{-}F/wt}$ vs *App* $^{NL\text{-}G\text{-}F/NL\text{-}G\text{-}F}$: t(16.214)=4.149, *P*=0.002, 95% CI: -0.032, -0.007 12 months: WT vs *App* $^{NL\text{-}G\text{-}F/wt}$: t(18.679)=0.556, *P*=0.845, 95% CI: -0.017,0.011 WT vs *App* $^{NL\text{-}G\text{-}F/NL\text{-}G\text{-}F}$: t(20.949)=6.185, *P*=0.000, 95% CI: -0.041,-0.017 *App* $^{NL\text{-}G\text{-}F/wt}$ vs *App* $^{NL\text{-}G\text{-}F/NL\text{-}G\text{-}F}$: t(20.816)=4.479, *P*=0.001, 95% CI:-0.040, -0.011

1E (Wake)	6-month-old mice: WT: n= 12 mice; *App* $^{NL\text{-}G\text{-}F/wt}$: n= 11 mice; *App* $^{NL\text{-}G\text{-}F/NL\text{-}G\text{-}F}$: n= 8 mice; 12-month-old mice: WT: n= 10 mice; *App* $^{NL\text{-}G\text{-}F/wt}$: n= 12 mice; *App* $^{NL\text{-}G\text{-}F/NL\text{-}G\text{-}F}$: n= 13 mice	n.a.	6 months: WT vs *App* $^{NL\text{-}G\text{-}F/wt}$: t(20.207)=1.878, *P*=0.171, 95% CI: -12.400, 84.090 WT vs *App* $^{NL\text{-}G\text{-}F/NL\text{-}G\text{-}F}$: t(10.617)=0.577, *P*=0.835, 95% CI: -58.802,90.546 *App* $^{NL\text{-}G\text{-}F/wt}$ vs *App* $^{NL\text{-}G\text{-}F/NL\text{-}G\text{-}F}$: t(11.728)=0.701, *P*=0.767, 95% CI: -96.188, 56.243 12 months: WT vs *App* $^{NL\text{-}G\text{-}F/wt}$: t(20.000)=0.668, *P*=0.785, 95% CI: -75.033,43.704 WT vs *App* $^{NL\text{-}G\text{-}F/NL\text{-}G\text{-}F}$: t(19.336)=2.047, *P*=0.128, 95% CI: -10.192,95.475 *App* $^{NL\text{-}G\text{-}F/wt}$ vs *App* $^{NL\text{-}G\text{-}F/NL\text{-}G\text{-}F}$: t(21.284)=2.643, *P*=0.039, 95% CI:2.756, 113.856
1E (NREMS)		n.a.	6 months: WT vs *App* $^{NL\text{-}G\text{-}F/wt}$: t(20.055)=1.917, *P*=0.160, 95% CI: -77.785, 10.708 WT vs *App* $^{NL\text{-}G\text{-}F/NL\text{-}G\text{-}F}$: t(10.480)=0.605, *P*=0.821, 95% CI: -84.219,53.597 *App* $^{NL\text{-}G\text{-}F/wt}$ vs *App* $^{NL\text{-}G\text{-}F/NL\text{-}G\text{-}F}$: t(11.723)=0.692, *P*=0.772, 95% CI: -52.238, 88.693 12 months: WT vs *App* $^{NL\text{-}G\text{-}F/wt}$: t(19.967)=0.591, *P*=0.826, 95% CI: -43.035,69.269 WT vs *App* $^{NL\text{-}G\text{-}F/NL\text{-}G\text{-}F}$: t(19.797)=2.096, *P*=0.116, 95% CI: -90.720,8.556 *App* $^{NL\text{-}G\text{-}F/wt}$ vs *App* $^{NL\text{-}G\text{-}F/NL\text{-}G\text{-}F}$: t(21.304)=2.545, *P*=0.047, 95% CI:-107.825, -0.572

1E (REMS)	6-month-old mice: WT: n= 12 mice; *App* $^{NL\text{-}G\text{-}F/wt}$: n= 11 mice; *App* $^{NL\text{-}G\text{-}F/NL\text{-}G\text{-}F}$: n= 8 mice; 12-month-old mice: WT: n= 10 mice; *App* $^{NL\text{-}G\text{-}F/wt}$: n= 12 mice; *App* $^{NL\text{-}G\text{-}F/NL\text{-}G\text{-}F}$: n= 13 mice	n.a.	6 months: WT vs *App* $^{NL\text{-}G\text{-}F/wt}$: t(20.706)=0.931, *P*=0.627, 95% CI: -8.557, 3.944 WT vs *App* $^{NL\text{-}G\text{-}F/NL\text{-}G\text{-}F}$: t(12.809)=0.182, *P*=0.982, 95% CI: -8.702,7.580 *App* $^{NL\text{-}G\text{-}F/wt}$ vs *App* $^{NL\text{-}G\text{-}F/NL\text{-}G\text{-}F}$: t(13.368)=0.554, *P*=0.846, 95% CI: -6.538, 10.029 12 months: WT vs *App* $^{NL\text{-}G\text{-}F/wt}$: t(19.442)=1.072, *P*=0.542, 95% CI: -3.480,8.576 WT vs *App* $^{NL\text{-}G\text{-}F/NL\text{-}G\text{-}F}$: t(13.128)=0.977, *P*=0.603, 95% CI: -5.768,2.649 *App* $^{NL\text{-}G\text{-}F/wt}$ vs *App* $^{NL\text{-}G\text{-}F/NL\text{-}G\text{-}F}$: t(13.910)=2.037, *P*=0.140, 95% CI:-9.387, 1.173
1E (REMS/Total sleep ratio)		n.a.	6 months: WT vs *App* $^{NL\text{-}G\text{-}F/wt}$: t(19.372)=0.295, *P*=0.953, 95% CI: -0.023, 0.018 WT vs *App* $^{NL\text{-}G\text{-}F/NL\text{-}G\text{-}F}$: t(11.661)=0.014, *P*=1.000, 95% CI: -0.027,0.027 *App* $^{NL\text{-}G\text{-}F/wt}$ vs *App* $^{NL\text{-}G\text{-}F/NL\text{-}G\text{-}F}$: t(13.888)=0.211, *P*=0.976, 95% CI: -0.026, 0.031 12 months: WT vs *App* $^{NL\text{-}G\text{-}F/wt}$: t(16.774)=1.262, *P*=0.435, 95% CI: -0.011, 0.031 WT vs *App* $^{NL\text{-}G\text{-}F/NL\text{-}G\text{-}F}$: t(17.319)=0.031, *P*=0.999, 95% CI: -0.012, 0.012 *App* $^{NL\text{-}G\text{-}F/wt}$ vs *App* $^{NL\text{-}G\text{-}F/NL\text{-}G\text{-}F}$: t(14.415)=1.358, *P*=0.388, 95% CI:-0.030,0.010

1F (Wake)	6-month-old mice: WT: n= 12 mice; *App* $^{NL\text{-}G\text{-}F/wt}$: n= 11 mice; *App* $^{NL\text{-}G\text{-}F/NL\text{-}G\text{-}F}$: n= 8 mice; 12-month-old mice: WT: n= 10 mice; *App* $^{NL\text{-}G\text{-}F/wt}$: n= 12 mice; *App* $^{NL\text{-}G\text{-}F/NL\text{-}G\text{-}F}$: n= 13 mice	n.a.	6 months: WT vs *App* $^{NL\text{-}G\text{-}F/wt}$: t(20.888)=1.624, *P*=0.258, 95% CI: -123.091, 26.667 WT vs *App* $^{NL\text{-}G\text{-}F/NL\text{-}G\text{-}F}$: t(15.519)=2.773, *P*=0.035, 95% CI: -184.733, -6.350 *App* $^{NL\text{-}G\text{-}F/wt}$ vs *App* $^{NL\text{-}G\text{-}F/NL\text{-}G\text{-}F}$: t(13.961)=1.440, *P*=0.349, 95% CI: -133.404, 38.745 12 months: WT vs *App* $^{NL\text{-}G\text{-}F/wt}$: t(18.040)=0.438, *P*=0.900, 95% CI: -104.535, 73.902 WT vs *App* $^{NL\text{-}G\text{-}F/NL\text{-}G\text{-}F}$: t(19.341)=2.317, *P*=0.077, 95% CI: -175.597, 7.951 *App* $^{NL\text{-}G\text{-}F/wt}$ vs *App* $^{NL\text{-}G\text{-}F/NL\text{-}G\text{-}F}$: t(22.963)=2.134, *P*=0.105, 95% CI:-148.895, 11.882
1F (NREMS)		n.a.	6 months: WT vs *App* $^{NL\text{-}G\text{-}F/wt}$: t(20.396)=1.551, *P*=0.289, 95% CI: -126.873, 30.327 WT vs *App* $^{NL\text{-}G\text{-}F/NL\text{-}G\text{-}F}$: t(17.237)=2.583, *P*=0.048, 95% CI: -175.296, -0.704 *App* $^{NL\text{-}G\text{-}F/wt}$ vs *App* $^{NL\text{-}G\text{-}F/NL\text{-}G\text{-}F}$: t(14.797)=1.290, *P*=0.422, 95% CI: -119.834, 40.379 12 months: WT vs *App* $^{NL\text{-}G\text{-}F/wt}$: t(19.652)=0.520, *P*=0.863, 95% CI: -100.819, 66.485 WT vs *App* $^{NL\text{-}G\text{-}F/NL\text{-}G\text{-}F}$: t(20.511)=2.673, *P*=0.037, 95% CI: -173.525, -4.937 *App* $^{NL\text{-}G\text{-}F/wt}$ vs *App* $^{NL\text{-}G\text{-}F/NL\text{-}G\text{-}F}$: t(22.990)=2.194, *P*=0.094, 95% CI:-154.337, 10.208

1F (REMS)	6-month-old mice:
	WT:
	n= 12 mice;
	App $^{NL\text{-}G\text{-}F/wt}$:
	n= 11 mice;
	App $^{NL\text{-}G\text{-}F/NL\text{-}G\text{-}F}$:
	n= 8 mice;
	12-month-old mice:
	WT:
	n= 10 mice; *App* $^{NL\text{-}G\text{-}F/wt}$:
	n= 12 mice;
	App $^{NL\text{-}G\text{-}F/NL\text{-}G\text{-}F}$:
	n= 13 mice
		n.a.	6 months:
			WT vs *App* $^{NL\text{-}G\text{-}F/wt}$:
			t(16.191)=0.589, *P*=0.828, 95% CI: -20.745, 33.032
			WT vs *App* $^{NL\text{-}G\text{-}F/NL\text{-}G\text{-}F}$:
			t(17.152)=1.180, *P*=0.480, 95% CI: -27.626, 10.210
			App $^{NL\text{-}G\text{-}F/wt}$ vs *App* $^{NL\text{-}G\text{-}F/NL\text{-}G\text{-}F}$:
			t(15.334)=1.426, *P*=0.353, 95% CI: -41.851, 12.147
			12 months:
			WT vs *App* $^{NL\text{-}G\text{-}F/wt}$:
			t(16.965)=0.209, *P*=0.976, 95% CI: -27.211, 23.111
			WT vs *App* $^{NL\text{-}G\text{-}F/NL\text{-}G\text{-}F}$:
			t(11.198)=1.836, *P*=0.203, 95% CI: -38.227, 7.243
			App $^{NL\text{-}G\text{-}F/wt}$ vs *App* $^{NL\text{-}G\text{-}F/NL\text{-}G\text{-}F}$:
			t(15.998)=2.115, *P*=0.118, 95% CI:-29.839, 2.954

1G (Wake)	6-month-old mice:
	WT:
	n= 12 mice; *App* $^{NL\text{-}G\text{-}F/wt}$:
	n= 11 mice;
	App $^{NL\text{-}G\text{-}F/NL\text{-}G\text{-}F}$:
	n= 8 mice;
	12-month-old mice:
	WT:
	n= 10 mice;
	App $^{NL\text{-}G\text{-}F/wt}$:
	n= 12 mice;
	App $^{NL\text{-}G\text{-}F/NL\text{-}G\text{-}F}$:
	n= 13 mice
		n.a.	6 months:
			WT vs *App* $^{NL\text{-}G\text{-}F/wt}$:
			t(18.041)=1.806, *P*=0.196, 95% CI: -18.278, 106.868
			WT vs *App* $^{NL\text{-}G\text{-}F/NL\text{-}G\text{-}F}$:
			t(8.300)=1.961, *P*=0.182, 95% CI: -41.966, 229.966
			App $^{NL\text{-}G\text{-}F/wt}$ vs *App* $^{NL\text{-}G\text{-}F/NL\text{-}G\text{-}F}$:
			t(9.720)=0.991, *P*=0.599, 95% CI: -88.377, 187.786
			12 months:
			WT vs *App* $^{NL\text{-}G\text{-}F/wt}$:
			t(15.910)=0.462, *P*=0.890, 95% CI: -61.497, 88.297
			WT vs *App* $^{NL\text{-}G\text{-}F/NL\text{-}G\text{-}F}$:
			t(17.712)=3.149, *P*=0.015, 95% CI: -16.501, 158.607
			App $^{NL\text{-}G\text{-}F/wt}$ vs *App* $^{NL\text{-}G\text{-}F/NL\text{-}G\text{-}F}$:
			t(22.785)=2.071, *P*=0.118, 95% CI: -15.557, 163.865

1G (NREMS)	6-month-old mice:
	WT:
	n= 12 mice; *App* $^{NL\text{-}G\text{-}F/wt}$:
	n= 11 mice;
	App $^{NL\text{-}G\text{-}F/NL\text{-}G\text{-}F}$:
	n= 8 mice;
	12-month-old mice:
	WT:
	n= 10 mice;
	App $^{NL\text{-}G\text{-}F/wt}$:
	n= 12 mice;
	App $^{NL\text{-}G\text{-}F/NL\text{-}G\text{-}F}$:
	n= 13 mice
		n.a.	6 months:
			WT vs *App* $^{NL\text{-}G\text{-}F/wt}$:
			t(20.936)=0.639, *P*=0.800, 95% CI: -24.387, 40.948
			WT vs *App* $^{NL\text{-}G\text{-}F/NL\text{-}G\text{-}F}$:
			t(13.966)=2.196, *P*=0.107, 95% CI: -6.525, 74.359
			App $^{NL\text{-}G\text{-}F/wt}$ vs *App* $^{NL\text{-}G\text{-}F/NL\text{-}G\text{-}F}$:
			t(13.829)=1.655, *P*=0.257, 95% CI: -14.960, 66.233
			12 months:
			WT vs *App* $^{NL\text{-}G\text{-}F/wt}$:
			t(19.761)=0.962, *P*=0.609, 95% CI: -10.751, 23.917
			WT vs *App* $^{NL\text{-}G\text{-}F/NL\text{-}G\text{-}F}$:
			t(20.555)=1.977, *P*=0.143, 95% CI: -3.762, 30.916
			App $^{NL\text{-}G\text{-}F/wt}$ vs *App* $^{NL\text{-}G\text{-}F/NL\text{-}G\text{-}F}$:
			t(22.969)=1.023, *P*=0.570, 95% CI: -10.126, 24.113

1G (REMS)		n.a.	6 months: WT vs *App* $^{NL\text{-}G\text{-}F/wt}$: t(19.779)=0.874, *P*=0.663, 95% CI: -8.513, 4.145 WT vs *App* $^{NL\text{-}G\text{-}F/NL\text{-}G\text{-}F}$: t(11.565)=0.929, *P*=0.634, 95% CI: -11.468, 5.568 *App* $^{NL\text{-}G\text{-}F/wt}$ vs *App* $^{NL\text{-}G\text{-}F/NL\text{-}G\text{-}F}$: t(13.343)=0.227, *P*=0.972, 95% CI: -9.631, 8.099 12 months: WT vs *App* $^{NL\text{-}G\text{-}F/wt}$: t(19.968)=0.109, *P*=0.993, 95% CI: -3.728, 4.065 WT vs *App* $^{NL\text{-}G\text{-}F/NL\text{-}G\text{-}F}$: t(20.880)=3.768, *P*=0.003, 95% CI: -9.305, -1.844 *App* $^{NL\text{-}G\text{-}F/wt}$ vs *App* $^{NL\text{-}G\text{-}F/NL\text{-}G\text{-}F}$: t(22.694)=3.618, *P*=0.004, 95% CI: -9.722, -1.764

1H (REMS latency)	6-month-old mice: WT : n= 12 mice; *App* $^{NL-G-F/wt}$: n= 11 mice; *App* $^{NL-G-F/NL-G-F}$: n= 8 mice; 12-month-old mice: WT : n= 10 mice; *App* $^{NL-G-F/wt}$: n= 12 mice; *App* $^{NL-G-F/NL-G-F}$: n= 13 mice	n.a.	6 months: WT vs *App* $^{NL-G-F/wt}$: t(20.215)=0.666, *P*=0.786, 95% CI: -30.097, 17.549 WT vs *App* $^{NL-G-F/NL-G-F}$: t(16.265)=1.805, *P*=0.199, 95% CI: -7.052, 40.058 *App* $^{NL-G-F/wt}$ vs *App* $^{NL-G-F/NL-G-F}$: t(16.740)=2.314, *P*=0.081, 95% CI: -2.506, 48.061 12 months: WT vs *App NL-G-F/wt*: t(19.990)=0.249, *P*=0.966, 95% CI: -12.684, 15.458 WT vs *App* $^{NL-G-F/NL-G-F}$: t(20.620)=0.745, *P*=0.740, 95% CI: -10.905, 20.033 *App* $^{NL-G-F/wt}$ vs *App* $^{NL-G-F/NL-G-F}$: t(22.690)=0.494, *P*=0.875, 95% CI: -12.941, 19.295

Supplementary Table 2.Detailed results of the statistical analyses in Figure 2.

Figure number	Sample size (n)	Games-Howell

2C (Wake)	6-month-old mice:
	WT:
	n= 12 mice;
	App $^{NL\text{-}G\text{-}F/}$:
	n= 11 mice;
	App $^{NL\text{-}G\text{-}F/NL\text{-}G\text{-}F}$:
	n= 8 mice;
	12-month-old mice:
	WT :
	n= 10 mice;
	App $^{NL\text{-}G\text{-}F/wt}$:
	n= 12 mice;
	App $^{NL\text{-}G\text{-}F/NL\text{-}G\text{-}F}$:
	n= 13 mice
		6 months:
		WT vs App $^{NL\text{-}G\text{-}F/wt}$:
		t(14.968)=0.255, *P*=0.965, 95% CI: -2.747, 3.343
		WT vs *App* $^{NL\text{-}G\text{-}F/NL\text{-}G\text{-}F}$:
		t(12.634)=3.685, *P*=0.008, 95% CI: 1.019, 6.233
		App $^{NL\text{-}G\text{-}F/wt}$ vs *App* $^{NL\text{-}G\text{-}F/NL\text{-}G\text{-}F}$:
		t(16.952)=2.498, *P*=0.057, 95% CI: -0.090, 6.745
		12 months:
		WT vs *App* $^{NL\text{-}G\text{-}F/wt}$:
		t(19.907)=0.456, *P*=0.892, 95% CI: -2.249, 3.238
		WT vs *App* $^{NL\text{-}G\text{-}F/NL\text{-}G\text{-}F}$:
		t(20.780)=4.853, *P*=0.000, 95% CI: -2.652, 8.391
		App $^{NL\text{-}G\text{-}F/wt}$ vs *App* $^{NL\text{-}G\text{-}F/NL\text{-}G\text{-}F}$:
		t(22.970)=4.116, *P*=0.001, 95% CI: -1.968, 8.086

2D (NREMS)	6-month-old mice:
	WT:
	n= 12 mice;
	App $^{NL\text{-}G\text{-}F/wt}$:
	n= 11 mice;
	App $^{NL\text{-}G\text{-}F/NL\text{-}G\text{-}F}$:
	n= 8 mice;
	12-month-old mice:
	WT:
	n= 10 mice;
	App $^{NL\text{-}G\text{-}F/wt}$:
	n= 12 mice;
	App $^{NL\text{-}G\text{-}F/NL\text{-}G\text{-}F}$:
	n= 13 mice
		6 months:
		WT vs *App* $^{NL\text{-}G\text{-}F/wt}$:
		t(20.319)=1.601, *P*=0.268, 95% CI: -8.264, 1.854
		WT vs *App* $^{NL\text{-}G\text{-}F/NL\text{-}G\text{-}F}$:
		t(18.000)=1.776, *P*=0.206, 95% CI: -8.680, 1.557
		App $^{NL\text{-}G\text{-}F/wt}$ vs *App* $^{NL\text{-}G\text{-}F/NL\text{-}G\text{-}F}$:
		t(16.445)=0.202, *P*=0.978, 95% CI: -4.886, 4.173
		12 months:
		WT vs *App* $^{NL\text{-}G\text{-}F/wt}$:
		t(19.999)=1.958, *P*=0.149, 95% CI: -0.745, 5.851
		WT vs *App* $^{NL\text{-}G\text{-}F/NL\text{-}G\text{-}F}$:
		t(20.174)=5.358, *P*=0.000, 95% CI: 4.306, 12.001
		App $^{NL\text{-}G\text{-}F/wt}$ vs *App* $^{NL\text{-}G\text{-}F/NL\text{-}G\text{-}F}$:
		t(22.083)=3.546, *P*=0.005, 95% CI: 1.634, 9.567

2E (REMS)	6-month-old mice:
	WT:
	n= 12 mice;
	App $^{NL\text{-}G\text{-}F/wt}$
	: n= 11 mice;
	App $^{NL\text{-}G\text{-}F/NL\text{-}G\text{-}F}$:
	n= 8 mice;
	12-month-old mice:
	WT:
	n= 10 mice;
	App $^{NL\text{-}G\text{-}F/wt}$:
	n= 12 mice;
	App $^{NL\text{-}G\text{-}F/NL\text{-}G\text{-}F}$:
	n= 13 mice
		6 months:
		WT vs *App* $^{NL\text{-}G\text{-}F/wt}$:
		t(20.837)=1.045, *P*=0.558, 95% CI: -1.676, 0.694
		WT vs *App* $^{NL\text{-}G\text{-}F/NL\text{-}G\text{-}F}$:
		t(13.042)=3.477, *P*=0.011, 95% CI: 0.533, 3.887
		App $^{NL\text{-}G\text{-}F/wt}$ vs *App* $^{NL\text{-}G\text{-}F/NL\text{-}G\text{-}F}$:
		t(11.660)=4.417, *P*=0.002, 95% CI: 1.063, 4.338
		12 months:
		WT vs *App* $^{NL\text{-}G\text{-}F/wt}$:
		t(18.868)=0.501, *P*=0.861, 95% CI: -1.591, 2.417
		WT vs *App* $^{NL\text{-}G\text{-}F/NL\text{-}G\text{-}F}$:
		t(19.745)=1.791, *P*=0.005, 95% CI: 1.152, 6.630
		App $^{NL\text{-}G\text{-}F/wt}$ vs *App* $^{NL\text{-}G\text{-}F/NL\text{-}G\text{-}F}$:
		t(18.918)=2.389, *P*=0.009, 95% CI: 0.836, 6.120

2F (Wake)	6-month-old mice:
	WT:
	n= 12 mice;
	App $^{NL\text{-}G\text{-}F/wt}$:
	n= 11 mice;
	App $^{NL\text{-}G\text{-}F/NL\text{-}G\text{-}F}$:
	n= 8 mice;
	12-month-old mice:
	WT:
	n= 10 mice;
	App $^{NL\text{-}G\text{-}F/wt}$:
	n= 12 mice;
	App $^{NL\text{-}G\text{-}F/NL\text{-}G\text{-}F}$:
	n= 13 mice
		6 months:
		WT vs *App* $^{NL\text{-}G\text{-}F/wt}$:
		t(14.525)=1.897, *P*=0.175, 95% CI: -0.590, 3.747
		WT vs *App* $^{NL\text{-}G\text{-}F/NL\text{-}G\text{-}F}$:
		t(8.971)=1.514, *P*=0.330, 95% CI: -1.330, 4.476
		App $^{NL\text{-}G\text{-}F/wt}$ vs *App* $^{NL\text{-}G\text{-}F/NL\text{-}G\text{-}F}$:
		t(14.240)=0.004, *P*=1.000, 95% CI: -3.214, 3.203
		12 months:
		WT vs *App* $^{NL\text{-}G\text{-}F/wt}$:
		t(16.838)=0.866, *P*=0.668, 95% CI: -3.896, 1.930
		WT vs *App* $^{NL\text{-}G\text{-}F/NL\text{-}G\text{-}F}$:
		t(14.927)=0.346, *P*=0.936, 95% CI: -2.417, 3.160
		App $^{NL\text{-}G\text{-}F/wt}$ vs *App* $^{NL\text{-}G\text{-}F/NL\text{-}G\text{-}F}$:
		t(21.832)=1.590, *P*=0.271, 95% CI: -0.786, 3.494

2G (NREMS)	6-month-old mice:
	WT:
	n= 12 mice;
	App $^{NL\text{-}G\text{-}F/wt}$:
	n= 11 mice;
	App $^{NL\text{-}G\text{-}F/NL\text{-}G\text{-}F}$:
	n= 8 mice;
	12-month-old mice:
	WT:
	n= 10 mice;
	App $^{NL\text{-}G\text{-}F/wt}$:
	n= 12 mice;
	App $^{NL\text{-}G\text{-}F/NL\text{-}G\text{-}F}$:
	n= 13 mice
		6 months:
		WT vs *App* $^{NL\text{-}G\text{-}F/wt}$:
		t(17.754)=0.478, *P*=0.883, 95% CI: -2.133, 3.085
		WT vs *App* $^{NL\text{-}G\text{-}F/NL\text{-}G\text{-}F}$:
		t(14.074)=2.892, *P*=0.030, 95% CI: -5.248, -0.264
		App $^{NL\text{-}G\text{-}F/wt}$ vs *App* $^{NL\text{-}G\text{-}F/NL\text{-}G\text{-}F}$:
		t(16.892)=2.843, *P*=0.029, 95% CI: -6.169, -0.315
		12 months:
		WT vs *App* $^{NL\text{-}G\text{-}F/wt}$:
		t(18.614)=0.983, *P*=0.596, 95% CI: -3.749, 1.660
		WT vs *App* $^{NL\text{-}G\text{-}F/NL\text{-}G\text{-}F}$:
		t(20.994)=6.260, *P*=0.000, 95% CI: -7.911, -3.369
		App $^{NL\text{-}G\text{-}F/wt}$ vs *App* $^{NL\text{-}G\text{-}F/NL\text{-}G\text{-}F}$:
		t(21.081)=4.142, *P*=0.001, 95% CI:-7.391, -1.800

2H (REMS)	6-month-old mice:
	WT:
	n= 12 mice;
	App $^{NL\text{-}G\text{-}F/wt}$:
	n= 11 mice;
	App $^{NL\text{-}G\text{-}F/NL\text{-}G\text{-}F}$: n= 8 mice;
	12-month-old mice:
	WT:
	n= 10 mice;
	App $^{NL\text{-}G\text{-}F/wt}$:
	n= 12 mice;
	App $^{NL\text{-}G\text{-}F/NL\text{-}G\text{-}F}$:
	n= 13 mice
		6 months:
		WT vs *App* $^{NL\text{-}G\text{-}F/wt}$:
		t(19.257)=0.988, *P*=0.593, 95% CI: -3.898, 8.868
		WT vs *App* $^{NL\text{-}G\text{-}F/NL\text{-}G\text{-}F}$:
		t(13.675)=0.773, *P*=0.725, 95% CI: -4.904, 8.997
		App $^{NL\text{-}G\text{-}F/wt}$ vs *App* $^{NL\text{-}G\text{-}F/NL\text{-}G\text{-}F}$:
		t(15.921)=0.149, *P*=0.988, 95% CI: -8.015, 7.138
		12 months:
		WT vs *App* $^{NL\text{-}G\text{-}F/wt}$:
		t(13.613)=0.308, *P*=0.949, 95% CI: -6.070, 4.797
		WT vs *App* $^{NL\text{-}G\text{-}F/NL\text{-}G\text{-}F}$:
		t(20.172)=2.974, *P*=0.020, 95% CI: -13.924, -1.128
		App $^{NL\text{-}G\text{-}F/wt}$ vs *App* $^{NL\text{-}G\text{-}F/NL\text{-}G\text{-}F}$:
		t(18.414)=3.483, *P*=0.007, 95% CI:-11.929, -1.851

2I (Wake)	6-month-old mice:
	WT:
	n= 12 mice;
	App $^{NL\text{-}G\text{-}F/wt}$:
	n= 11 mice;
	App $^{NL\text{-}G\text{-}F/NL\text{-}G\text{-}F}$:
	n= 8 mice;
	12-month-old mice:
	WT:
	n= 10 mice;
	App $^{NL\text{-}G\text{-}F/wt}$:
	n= 12 mice;
	App $^{NL\text{-}G\text{-}F/NL\text{-}G\text{-}F}$:
	n= 13 mice
		6 months:
		WT vs *App* $^{NL\text{-}G\text{-}F/wt}$:
		t(20.101)=1.266, *P*=0.430, 95% CI: -0.154, 0.463
		WT vs *App* $^{NL\text{-}G\text{-}F/NL\text{-}G\text{-}F}$:
		t(8.650)=0.312, *P*=0.948, 95% CI: -0.612, 0.764
		App $^{NL\text{-}G\text{-}F/wt}$ vs *App* $^{NL\text{-}G\text{-}F/NL\text{-}G\text{-}F}$:
		t(9.280)=0.314, *P*=0.947, 95% CI: -0.771, 0.614
		12 months:
		WT vs *App* $^{NL\text{-}G\text{-}F/wt}$:
		t(19.188)=0.343, *P*=0.937, 95% CI: -0.360, 0.274
		WT vs *App* $^{NL\text{-}G\text{-}F/NL\text{-}G\text{-}F}$:
		t(20.982)=1.128, *P*=0.508, 95% CI: -0.201, 0.526
		App $^{NL\text{-}G\text{-}F/wt}$ vs *App* $^{NL\text{-}G\text{-}F/NL\text{-}G\text{-}F}$:
		t(21.858)=1.485, *P*=0.317, 95% CI:-0.142, 0.554

2J (NREMS)	6-month-old mice:
	WT:
	n= 12 mice;
	App $^{NL\text{-}G\text{-}F/wt}$:
	n= 11 mice;
	App $^{NL\text{-}G\text{-}F/NL\text{-}G\text{-}F}$:
	n= 8 mice;
	12-month-old mice:
	WT:
	n= 10 mice;
	App $^{NL\text{-}G\text{-}F/wt}$:
	n= 12 mice;
	App $^{NL\text{-}G\text{-}F/NL\text{-}G\text{-}F}$:
	n= 13 mice
		6 months:
		WT vs *App* $^{NL\text{-}G\text{-}F/wt}$:
		t(20.987)=0.631, *P*=0.805, 95% CI: -0.107, 0.179
		WT vs *App* $^{NL\text{-}G\text{-}F/NL\text{-}G\text{-}F}$:
		t(9.718)=1.886, *P*=0.194, 95% CI: -0.480, 0.090
		App $^{NL\text{-}G\text{-}F/wt}$ vs *App* $^{NL\text{-}G\text{-}F/NL\text{-}G\text{-}F}$:
		t(9.338)=2.257, *P*=0.113, 95% CI: -0.514, 0.053
		12 months:
		WT vs *App* $^{NL\text{-}G\text{-}F/wt}$:
		t(19.248)=0.501, *P*=0.031, 95% CI: -0.374, -0.017
		WT vs *App* $^{NL\text{-}G\text{-}F/NL\text{-}G\text{-}F}$:
		t(16.414)=1.791, *P*=0.000, 95% CI: -0.628, -0.304
		App $^{NL\text{-}G\text{-}F/wt}$ vs *App* $^{NL\text{-}G\text{-}F/NL\text{-}G\text{-}F}$:
		t(20.638)=2.389, *P*=0.000, 95% CI:-0.419, -0..122

2K (REMS)	6-month-old mice:
	WT:
	n= 12 mice;
	App $^{NL\text{-}G\text{-}F/wt}$:
	n= 11 mice;
	App $^{NL\text{-}G\text{-}F/NL\text{-}G\text{-}F}$:
	n= 8 mice;
	12-month-old mice:
	WT:
	n= 10 mice;
	App $^{NL\text{-}G\text{-}F/wt}$:
	n= 12 mice;
	App $^{NL\text{-}G\text{-}F/NL\text{-}G\text{-}F}$:
	n= 13 mice
		6 months:
		WT vs *App* $^{NL\text{-}G\text{-}F/wt}$:
		t(20.708)=0.1.527, *P*=0.299, 95% CI: -0.191, 0.047
		WT vs *App* $^{NL\text{-}G\text{-}F/NL\text{-}G\text{-}F}$:
		t(9.135)=2.318, *P*=0.103, 95% CI: -0.508, 0.046
		App $^{NL\text{-}G\text{-}F/wt}$ vs *App* $^{NL\text{-}G\text{-}F/NL\text{-}G\text{-}F}$:
		t(8.519)=1.625, *P*=0.287, 95% CI: -0.434, 0.117
		12 months:
		WT vs *App* $^{NL\text{-}G\text{-}F/wt}$:
		t(16.272)=2.219, *P*=0.098, 95% CI: -0.311, 0.023
		WT vs *App* $^{NL\text{-}G\text{-}F/NL\text{-}G\text{-}F}$:
		t(15.308)=6.751, *P*=0.000, 95% CI: -0.588, -0.262
		App $^{NL\text{-}G\text{-}F/wt}$ vs *App* $^{NL\text{-}G\text{-}F/NL\text{-}G\text{-}F}$:
		t(22.522)=5.760, *P*=0.000, 95% CI:-0.403, -0.159

2L (Wake)	6-month-old mice:
	WT:
	n= 12 mice;
	App $^{NL\text{-}G\text{-}F/wt}$:
	n= 11 mice;
	App $^{NL\text{-}G\text{-}F/NL\text{-}G\text{-}F}$:
	n= 8 mice;
	12-month-old mice:
	WT:
	n= 10 mice;
	App $^{NL\text{-}G\text{-}F/wt}$:
	n= 12 mice;
	App $^{NL\text{-}G\text{-}F/NL\text{-}G\text{-}F}$:
	n= 13 mice
		6 months:
		WT vs *App* $^{NL\text{-}G\text{-}F/wt}$:
		t(20.720)=1.244, *P*=0.442, 95% CI: -0.006, 0.017
		WT vs *App* $^{NL\text{-}G\text{-}F/NL\text{-}G\text{-}F}$:
		t(9.447)=0.994, *P*=0.598, 95% CI: -0.034, 0.016
		App $^{NL\text{-}G\text{-}F/wt}$ vs *App* $^{NL\text{-}G\text{-}F/NL\text{-}G\text{-}F}$:
		t(8.750)=1.654, *P*=0.275, 95% CI: -0.039, 0.010
		12 months:
		WT vs *App* $^{NL\text{-}G\text{-}F/wt}$:
		t(19.283)=0.412, *P*=0.911, 95% CI: -0.019, 0.013
		WT vs *App* $^{NL\text{-}G\text{-}F/NL\text{-}G\text{-}F}$:
		t(15.134)=1.535, *P*=0.303, 95% CI: -0.022, 0.006
		App $^{NL\text{-}G\text{-}F/wt}$ vs *App* $^{NL\text{-}G\text{-}F/NL\text{-}G\text{-}F}$:
		t(19.231)=1.129, *P*=0.508, 95% CI:-0.019, 0.007

2M (NREMS)	6-month-old mice:
	WT:
	n= 12 mice;
	App $^{NL\text{-}G\text{-}F/wt}$:
	n= 11 mice;
	App $^{NL\text{-}G\text{-}F/NL\text{-}G\text{-}F}$:
	n= 8 mice;
	12-month-old mice:
	WT:
	n= 10 mice;
	App $^{NL\text{-}G\text{-}F/wt}$:
	n= 12 mice;
	App $^{NL\text{-}G\text{-}F/NL\text{-}G\text{-}F}$:
	n= 13 mice
		6 months:
		WT vs *App* $^{NL\text{-}G\text{-}F/wt}$:
		t(20.824)=0.167, *P*=0.485, 95% CI: -0.002, 0.005
		WT vs *App* $^{NL\text{-}G\text{-}F/NL\text{-}G\text{-}F}$:
		t(12.270)=0.982, *P*=0.601, 95% CI: -0.007, 0.003
		App $^{NL\text{-}G\text{-}F/wt}$ vs *App* $^{NL\text{-}G\text{-}F/NL\text{-}G\text{-}F}$:
		t(9.418)=1.861, *P*=0.196, 95% CI: -0.009, 0.002
		12 months:
		WT vs *App* $^{NL\text{-}G\text{-}F/wt}$:
		t(18.129)=2.853, *P*=0.027, 95% CI: -0.008, 0.000
		WT vs *App* $^{NL\text{-}G\text{-}F/NL\text{-}G\text{-}F}$:
		t(13.580)=7.765, *P*=0.000, 95% CI: -0.013, -0.007
		App $^{NL\text{-}G\text{-}F/wt}$ vs *App* $^{NL\text{-}G\text{-}F/NL\text{-}G\text{-}F}$:
		t(18.869)=5.337, *P*=0.000, 95% CI:-0.009, -0.003

2N (REMS)	6-month-old mice:
	WT:
	n= 12 mice;
	App $^{NL\text{-}G\text{-}F/wt}$:
	n= 11 mice;
	App $^{NL\text{-}G\text{-}F/NL\text{-}G\text{-}F}$:
	n= 8 mice;
	12-month-old mice:
	WT:
	n= 10 mice;
	App $^{NL\text{-}G\text{-}F/wt}$:
	n= 12 mice;
	App $^{NL\text{-}G\text{-}F/NL\text{-}G\text{-}F}$:
	n= 13 mice
		6 months:
		WT vs *App* $^{NL\text{-}G\text{-}F/wt}$:
		t(20.222)=0.349, *P*=0.935, 95% CI: -0.017, 0.013
		WT vs *App* $^{NL\text{-}G\text{-}F/NL\text{-}G\text{-}F}$:
		t(10.956)=3.317, *P*=0.017, 95% CI: -0.061, -0.006
		App $^{NL\text{-}G\text{-}F/wt}$ vs *App* $^{NL\text{-}G\text{-}F/NL\text{-}G\text{-}F}$:
		t(9.418)=3.253, *P*=0.023, 95% CI: -0.059, -0.005
		12 months:
		WT vs *App* $^{NL\text{-}G\text{-}F/wt}$:
		t(17.087)=1.696, *P*=0.235, 95% CI: -0.037, 0.008
		WT vs *App* $^{NL\text{-}G\text{-}F/NL\text{-}G\text{-}F}$:
		t(13.162)=6.634, *P*=0.000, 95% CI: -0.072, -0.031
		App $^{NL\text{-}G\text{-}F/wt}$ vs *App* $^{NL\text{-}G\text{-}F/NL\text{-}G\text{-}F}$:
		t(19.437)=6.051, *P*=0.000, 95% CI:-0.053, -0.022

2O (REMS)	6-month-old mice:
	WT:
	n= 12 mice;
	App $^{NL\text{-}G\text{-}F/wt}$:
	n= 11 mice;
	App $^{NL\text{-}G\text{-}F/NL\text{-}G\text{-}F}$:
	n= 8 mice;
	12-month-old mice:
	WT:
	n= 10 mice;
	App $^{NL\text{-}G\text{-}F/wt}$:
	n= 12 mice;
	App $^{NL\text{-}G\text{-}F/NL\text{-}G\text{-}F}$:
	n= 13 mice
		6 months:
		WT vs *App* $^{NL\text{-}G\text{-}F/wt}$:
		t(19.669)=1.314, *P*=0.404, 95% CI: -0.359, 1.134
		WT vs *App* $^{NL\text{-}G\text{-}F/NL\text{-}G\text{-}F}$:
		t(15.990)=1.647, *P*=0.256, 95% CI: -1.181, 0.261
		App $^{NL\text{-}G\text{-}F/wt}$ vs *App* $^{NL\text{-}G\text{-}F/NL\text{-}G\text{-}F}$:
		t(16.873)=2.728, *P*=0.036, 95% CI: -1.645, -0.050
		12 months:
		WT vs *App* $^{NL\text{-}G\text{-}F/wt}$:
		t(14.488)=0.589, *P*=0.828, 95% CI: -1.116, 0.704
		WT vs *App* $^{NL\text{-}G\text{-}F/NL\text{-}G\text{-}F}$:
		t(13.438)=3.976, *P*=0.004, 95% CI: -2.243, -0.457
		App $^{NL\text{-}G\text{-}F/wt}$ vs *App* $^{NL\text{-}G\text{-}F/NL\text{-}G\text{-}F}$:
		t(22.371)=4.985, *P*=0.000, 95% CI: -1.720, -0.568

Supplementary Table 3. Detailed results of the statistical analyses in Figure 3.

Figure number	Sample size (n)	Games-Howell

3A(Wake)	6-month-old mice:
	WT:
	n= 12 mice;
	App $^{NL\text{-}G\text{-}F/wt}$:
	n= 11 mice;
	8 *App* $^{NL\text{-}G\text{-}F/NL\text{-}G\text{-}F}$:
	n= 8 mice;
	12-month-old mice:
	WT:
	n= 10 mice;
	App $^{NL\text{-}G\text{-}F/wt}$:
	n= 12 mice;
	App $^{NL\text{-}G\text{-}F/NL\text{-}G\text{-}F}$:
	n= 13 mice
		6 months:
		WT vs *App* $^{NL\text{-}G\text{-}F/wt}$:
		t(18.854)=2.140, *P*=0.108 95% CI: -23.977, 2.059
		WT vs *App* $^{NL\text{-}G\text{-}F/NL\text{-}G\text{-}F}$:
		t(9.620)=0.396, *P*=0.918, 95% CI: -24.377, 18.260
		App $^{NL\text{-}G\text{-}F/wt}$ vs *App* $^{NL\text{-}G\text{-}F/NL\text{-}G\text{-}F}$:
		t(11.574)=0.963, *P*=0.613, 95% CI: -14.092, 29.893
		12 months:
		WT vs *App* $^{NL\text{-}G\text{-}F/wt}$:
		t(19.990)=1.251, *P*=0.438, 95% CI: -8.850, 26.168
		WT vs *App* $^{NL\text{-}G\text{-}F/NL\text{-}G\text{-}F}$:
		t(16.780)=0.965, *P*=0.608, 95% CI: -9.157, 20.186
		App $^{NL\text{-}G\text{-}F/wt}$ vs *App* $^{NL\text{-}G\text{-}F/NL\text{-}G\text{-}F}$:
		t(18.929)=0.521, *P*=0.862, 95% CI:-18.467, 12.179

3A (NREMS)		6 months: WT vs *App* $^{NL\text{-}G\text{-}F/wt}$: t(18.009)=2.246, *P*=0.090 95% CI: -1.474, 23.153 WT vs *App* $^{NL\text{-}G\text{-}F/NL\text{-}G\text{-}F}$: t(9.747)=1.021, *P*=0.581, 95% CI: -11.729, 25.562 *App* $^{NL\text{-}G\text{-}F/wt}$ vs *App* $^{NL\text{-}G\text{-}F/NL\text{-}G\text{-}F}$: t(12.474)=0.533, *P*=0.857, 95% CI: -23.471, 15.625 12 months: WT vs *App* $^{NL\text{-}G\text{-}F/wt}$: t(19.987)=1.160, *P*=0.490, 95% CI: -23.581, 8.754 WT vs *App* $^{NL\text{-}G\text{-}F/NL\text{-}G\text{-}F}$: t(16.756)=0.280, *P*=0.958, 95% CI: -14.624, 11.746 *App* $^{NL\text{-}G\text{-}F/wt}$ vs *App* $^{NL\text{-}G\text{-}F/NL\text{-}G\text{-}F}$: t(18.337)=1.065, *P*=0.547, 95% CI:-8.320, 20.269

3A (REMS)	6-month-old mice:
	WT:
	n= 12 mice;
	App $^{NL\text{-}G\text{-}F/wt}$:
	n= 11 mice;
	8 *App* $^{NL\text{-}G\text{-}F/NL\text{-}G\text{-}F}$:
	n= 8 mice;
	12-month-old mice:
	WT:
	n= 10 mice;
	App $^{NL\text{-}G\text{-}F/wt}$:
	n= 12 mice;
	App $^{NL\text{-}G\text{-}F/NL\text{-}G\text{-}F}$:
	n= 13 mice
		6 months:
		WT vs *App* $^{NL\text{-}G\text{-}F/wt}$:
		t(14.362)=0.098, *P*=0.995 95% CI: -2.934, 3.163
		WT vs *App* $^{NL\text{-}G\text{-}F/NL\text{-}G\text{-}F}$:
		t(9.106)=2.771, *P*=0.051, 95% CI: -7.749, 0.021
		App $^{NL\text{-}G\text{-}F/wt}$ vs *App* $^{NL\text{-}G\text{-}F/NL\text{-}G\text{-}F}$:
		t(14.764)=2.375, *P*=0.076, 95% CI: -8.336, 0.380
		12 months:
		WT vs *App* $^{NL\text{-}G\text{-}F/wt}$:
		t(19.906)=1.103, *P*=0.523, 95% CI: -4.103, 1.612
		WT vs *App* $^{NL\text{-}G\text{-}F/NL\text{-}G\text{-}F}$:
		t(20.531)=3.086, *P*=0.015, 95% CI: -7.411, -0.741
		App $^{NL\text{-}G\text{-}F/wt}$ vs *App* $^{NL\text{-}G\text{-}F/NL\text{-}G\text{-}F}$:
		t(21.938)=2.118, *P*=0.109, 95% CI:-6.187, 0.527

3A (REMS/Total sleep ratio)		6 months: WT vs *App* $^{NL\text{-}G\text{-}F/wt}$: t(12.762)=1.011, P=0.583 95% CI: -0.024, 0.011 WT vs *App* $^{NL\text{-}G\text{-}F/NL\text{-}G\text{-}F}$: t(8.559)=3.728, P=0.013, 95% CI: -0.047, -0.007 *App* $^{NL\text{-}G\text{-}F/wt}$ vs *App* $^{NL\text{-}G\text{-}F/NL\text{-}G\text{-}F}$: t(15.598)=2.221, P=0.099, 95% CI: -0.044, 0.003 12 months: WT vs *App* $^{NL\text{-}G\text{-}F/wt}$: t(19.074)=0.354, P=0.933, 95% CI: -0.017, 0.013 WT vs *App* $^{NL\text{-}G\text{-}F/NL\text{-}G\text{-}F}$: t(18.469)=3.217, P=0.012, 95% CI: -0.040, -0.005 *App* $^{NL\text{-}G\text{-}F/wt}$ vs *App* $^{NL\text{-}G\text{-}F/NL\text{-}G\text{-}F}$: t(22.250)=2.629, P=0.039, 95% CI:-0.039, -0.001

3B (Sleep latency)	6-month-old mice:
	WT:
	n= 12 mice;
	App $^{NL\text{-}G\text{-}F/wt}$:
	n= 11 mice;
	8 *App* $^{NL\text{-}G\text{-}F/NL\text{-}G\text{-}F}$:
	n= 8 mice;
	12-month-old mice:
	WT:
	n= 10 mice;
	App $^{NL\text{-}G\text{-}F/wt}$:
	n= 12 mice;
	App $^{NL\text{-}G\text{-}F/NL\text{-}G\text{-}F}$:
	n= 13 mice
		6 months:
		WT vs *App* $^{NL\text{-}G\text{-}F/wt}$:
		t(20.284)=0.485, *P*=0.879 95% CI: -17.143, 11.626
		WT vs *App* $^{NL\text{-}G\text{-}F/NL\text{-}G\text{-}F}$:
		t(11.881)=0.288, *P*=0.956, 95% CI: -25.900, 20.861
		App $^{NL\text{-}G\text{-}F/wt}$ vs *App* $^{NL\text{-}G\text{-}F/NL\text{-}G\text{-}F}$:
		t(10.062)=0.029, *P*=1.000, 95% CI: -22.504, 22.982
		12 months:
		WT vs *App* $^{NL\text{-}G\text{-}F/wt}$:
		t(19.167)=1.277, *P*=0.424, 95% CI: -7.938, 24.013
		WT vs *App* $^{NL\text{-}G\text{-}F/NL\text{-}G\text{-}F}$:
		t(19.226)=0.187, *P*=0.981, 95% CI: -16.771, 14.471
		App $^{NL\text{-}G\text{-}F/wt}$ vs *App* $^{NL\text{-}G\text{-}F/NL\text{-}G\text{-}F}$:
		t(22.795)=1.584, *P*=0.272, 95% CI:-23.719, 5.343

3C (REMS latency)	6-month-old mice:
	WT:
	n= 12 mice;
	App $^{NL\text{-}G\text{-}F/wt}$:
	n= 11 mice;
	8 *App* $^{NL\text{-}G\text{-}F/NL\text{-}G\text{-}F}$:
	n= 8 mice;
	12-month-old mice:
	WT:
	n= 10 mice;
	App $^{NL\text{-}G\text{-}F/wt}$:
	n= 12 mice;
	App $^{NL\text{-}G\text{-}F/NL\text{-}G\text{-}F}$:
	n= 13 mice
		6 months:
		WT vs *App* $^{NL\text{-}G\text{-}F/wt}$:
		t(18.783)=1.886, *P*=0.170 95% CI: -4.243, 0.629
		WT vs *App* $^{NL\text{-}G\text{-}F/NL\text{-}G\text{-}F}$:
		t(17.042)=2.875, *P*=0.027, 95% CI: -4.394, -0.251
		App $^{NL\text{-}G\text{-}F/wt}$ vs *App* $^{NL\text{-}G\text{-}F/NL\text{-}G\text{-}F}$:
		t(16.787)=0.536, *P*=855, 95% CI: -2.983, 1.953
		12 months:
		WT vs *App* $^{NL\text{-}G\text{-}F/wt}$:
		t(18.695)=1.075, *P*=0.540, 95% CI: -1.149, 2.831
		WT vs *App* $^{NL\text{-}G\text{-}F/NL\text{-}G\text{-}F}$:
		t(20.344)=0.132, *P*=0.990, 95% CI: -2.205, 1.985
		App $^{NL\text{-}G\text{-}F/wt}$ vs *App* $^{NL\text{-}G\text{-}F/NL\text{-}G\text{-}F}$:
		t(22.834)=1.240, *P*=0.442, 95% CI:-2.872, 0.970

Supplementary Table 4. Detailed results of the statistical analyses in Figure 4.

Figure number	Sample size (n)	Mixed ANOVA	Games-Howell
4A 7-month-old mice	WT: n= 12 mice; *App* $^{NL\text{-}G\text{-}F/wt}$: n= 9 mice; *App* $^{NL\text{-}G\text{-}F/NL\text{-}G\text{-}F}$: n= 8 mice	period: F(1, 26)= 214.701, P=0.000 period*genotype: F(2,26)= 0.501, P=0.612 genotype: F(2,26)= 0.715, P=0.499	n.a.
4A 13-month-old mice	WT: n= 9 mice; *App* $^{NL\text{-}G\text{-}F/wt}$: n= 10 mice; *App* $^{NL\text{-}G\text{-}F/NL\text{-}G\text{-}F}$: n= 11 mice	period: F(1,26)= 410.560 , P=0.000 period*genotype: F(2,28)= 410.560, P=0.309 genotype: F(2,28)= 0.807, P=0.456	n.a.
4B 7-month-old mice	WT: n= 12 mice; *App* $^{NL\text{-}G\text{-}F/wt}$: n= 9 mice; *App* $^{NL\text{-}G\text{-}F/NL\text{-}G\text{-}F}$: n= 8 mice	CS: F(4,104)= 36.555, P= 0.000 CS*genotype: F(8,104)= 1.041, P= 0.411 genotype: F(2,26)= 0.968, P=0.393	n.a.
4B 13-month-old mice	WT: n= 9 mice; *App* $^{NL\text{-}G\text{-}F/wt}$: n= 10 mice; *App* $^{NL\text{-}G\text{-}F/NL\text{-}G\text{-}F}$: n= 11 mice	CS: F(4,112)= 32.333, P= 0.000 CS*genotype: F(8,112)=2.976, P= 0.005 genotype : F(2,28)= 5.932, P=0.007	WT vs *App* $^{NL\text{-}G\text{-}F/wt}$: CS1: t(18.000)=0.787, *P*=0.716, 95% CI: -12.912, 24.415; CS2: t(17.584)=0.554, *P*=0.846, 95% CI: -28.907, 44.901; CS3: t(17.931)=0.646, *P*=0.797, 95% CI: -35.258, 21.013; CS4: t(15.013)=1.123, *P*=0.515, 95% CI: -42.412, 16.802; CS5: t(15.997)=3.065, *P*=0.019, 95% CI: -53.243, -4.570

4B
13-month-old mice
	WT:
	n= 9 mice;
	App $^{NL\text{-}G\text{-}F/wt}$:
	n= 10 mice;
	App $^{NL\text{-}G\text{-}F/NL\text{-}G\text{-}F}$:
	n= 11 mice
			WT vs *App* $^{NL\text{-}G\text{-}F/NL\text{-}G\text{-}F}$:
			CS1: t(17.242)=0.897, *P*=0.649, 95% CI: -13.955, 28.985; CS2: t(14.610)=1.514, *P*=0.313, 95% CI: -51.872, 13.739; CS3: t(17.809)=2.711, *P*=0.037, 95% CI: -63.816, -1.901; CS4: t(16.717)=4.693, *P*=0.001, 95% CI: -70.548, -20.626; CS5: t(13.965)=3.198, *P*=0.017, 95% CI: -67.503, -6.728
			App $^{NL\text{-}G\text{-}F/wt}$ vs *App* $^{NL\text{-}G\text{-}F/NL\text{-}G\text{-}F}$:
			CS1: t(19.072)=0.202, *P*=0.978, 95% CI:-20.363, 23.891
			CS2: t(18.026)=2.210, *P*=0.096, 95% CI: -58.309, 4.182
			CS3: t(19.462)=2.082, *P*=0.120, 95% CI: -57.085, 5.612
			CS4: t(19.126)=2.541, *P*=0.050, 95% CI: -65.537, -0.027
			CS5: t(18.731)=0.069, *P*=0.812, 95% CI: -41.941, 25.523

4C	7-month-old mice:
	WT:
	n= 12 mice; *App* $^{NL\text{-}G\text{-}F/wt}$:
	n= 9 mice; *App* $^{NL\text{-}G\text{-}F/NL\text{-}G\text{-}F}$:
	n= 8 mice;
	13-month-old mice:
	WT:
	n= 9 mice;
	App $^{NL\text{-}G\text{-}F/wt}$:
	n= 10 mice;
	App $^{NL\text{-}G\text{-}F/NL\text{-}G\text{-}F}$:
	n= 11 mice
		n.a.	7 months:
			WT vs *App* $^{NL\text{-}G\text{-}F/wt}$:
			t(17.146)=1.611, P=0.268 95% CI: -42.927, 9.788
			WT vs *App* $^{NL\text{-}G\text{-}F/NL\text{-}G\text{-}F}$:
			t(17.503)=2.645, P=0.042, 95% CI: -41.477, -0.689
			App $^{NL\text{-}G\text{-}F/wt}$ vs *App* $^{NL\text{-}G\text{-}F/NL\text{-}G\text{-}F}$:
			t(12.435)=0.501, P=0.872, 95% CI: -28.438, 19.410
			13 months:
			WT vs *App* $^{NL\text{-}G\text{-}F/wt}$:
			t(12.774)=0.993, P=0.594, 95% CI: -46.229, 21.001
			WT vs *App* $^{NL\text{-}G\text{-}F/NL\text{-}G\text{-}F}$:
			t(9.790)=2.093, P=0.142, 95% CI: -56.472, 7.674
			App $^{NL\text{-}G\text{-}F/wt}$ vs *App* $^{NL\text{-}G\text{-}F/NL\text{-}G\text{-}F}$:
			t(14.765)=1.622, P=0.267, 95% CI:-30.684, 7.114

Supplementary Table 5. Detailed results of the statistical analyses in Figure 5.

Figure number	Sample size (n)	Welch t-test
5I	7- and 13-month-old WT: n= 7 mice (control); 7-month-old mice: *App* $^{NL\text{-}G\text{-}F/wt}$: n= 3 mice; *App* $^{NL\text{-}G\text{-}F/NL\text{-}G\text{-}F}$: n= 5 mice; 13-month-old mice: *App* $^{NL\text{-}G\text{-}F/wt}$: n= 5 mice; *App* $^{NL\text{-}G\text{-}F/NL\text{-}G\text{-}F}$: n= 5 mice	6 months: *App* $^{NL\text{-}G\text{-}F/wt}$ vs *App* $^{NL\text{-}G\text{-}F/NL\text{-}G\text{-}F}$: t(4.043)=-2.737, P=0.051, 95% CI: -2.486, 0.013 12 months: *App* $^{NL\text{-}G\text{-}F/wt}$ vs App $^{NL\text{-}G\text{-}F/NL\text{-}G\text{-}F}$: t(5.408)=-0.584, P=0.583, 95% CI: -0.930, 0.580
5J	7- and 13-month-old WT: n= 7 mice (control); 7-month-old mice: *App* $^{NL\text{-}G\text{-}F/wt}$: n= 3 mice; *App* $^{NL\text{-}G\text{-}F/NL\text{-}G\text{-}F}$: n= 5 mice; 13-month-old mice: *App* $^{NL\text{-}G\text{-}F/wt}$: n= 5 mice; *App* $^{NL\text{-}G\text{-}F/NL\text{-}G\text{-}F}$: n= 6 mice	6 months: *App* $^{NL\text{-}G\text{-}F/wt}$ vs *App* $^{NL\text{-}G\text{-}F/NL\text{-}G\text{-}F}$: t(4.165)=-4.916, P=0.007, 95% CI: -2.019, -0.576 12 months: *App* $^{NL\text{-}G\text{-}F/wt}$ vs *App* $^{NL\text{-}G\text{-}F/NL\text{-}G\text{-}F}$: t(5.952)=-2.765, P=0.033, 95% CI:-2.759, -0.165
5K	7- and 13-month-old WT: n= 7 mice (control); 7-month-old mice: *App* $^{NL\text{-}G\text{-}F/wt}$: n= 3 mice; *App* $^{NL\text{-}G\text{-}F/NL\text{-}G\text{-}F}$: n= 5 mice; 13-month-old mice: *App* $^{NL\text{-}G\text{-}F/wt}$: n= 5 mice; *App* $^{NL\text{-}G\text{-}F/NL\text{-}G\text{-}F}$: n= 6 mice	6 months: *App* $^{NL\text{-}G\text{-}F/wt}$ vs *App* $^{NL\text{-}G\text{-}F/NL\text{-}G\text{-}F}$: t(4.502)=-3.089, P=0.031, 95% CI: -2.204, -0.165 12 months: *App* $^{NL\text{-}G\text{-}F/wt}$ vs *App* $^{NL\text{-}G\text{-}F/NL\text{-}G\text{-}F}$: t(8.989)=-1.295, P=0.228, 95% CI:-2.551, 0.694
5L	7- and 13-month-old WT: n= 6 mice (control); 7-month-old mice: *App* $^{NL\text{-}G\text{-}F/wt}$: n= 4 mice; *App* $^{NL\text{-}G\text{-}F/NL\text{-}G\text{-}F}$: n= 5 mice; 13-month-old mice: *App* $^{NL\text{-}G\text{-}F/wt}$: n= 4 mice; *App* $^{NL\text{-}G\text{-}F/NL\text{-}G\text{-}F}$: n= 6 mice	6 months: *App* $^{NL\text{-}G\text{-}F/wt}$ vs *App* $^{NL\text{-}G\text{-}F/NL\text{-}G\text{-}F}$: t(4.081)=-5.192, P=0.006, 95% CI: -0.352, -0.108 12 months: *App* $^{NL\text{-}G\text{-}F/wt}$ vs *App* $^{NL\text{-}G\text{-}F/NL\text{-}G\text{-}F}$: t(5.008)=-3.261, P=0.022, 95% CI:-1.867, 0.022
5M	7- and 13-month-old WT: n= 6 mice (control); 7-month-old mice: *App* $^{NL\text{-}G\text{-}F/wt}$: n= 4 mice; *App* $^{NL\text{-}G\text{-}F/NL\text{-}G\text{-}F}$: n= 5 mice; 13-month-old mice: *App* $^{NL\text{-}G\text{-}F/wt}$: n= 4 mice; *App* $^{NL\text{-}G\text{-}F/NL\text{-}G\text{-}F}$: n= 6 mice	6 months: *App* $^{NL\text{-}G\text{-}F/wt}$ vs *App* $^{NL\text{-}G\text{-}F/NL\text{-}G\text{-}F}$: t(5.377)=-2.422, P=0.056, 95% CI: -0.315, 0.070 12 months: *App* $^{NL\text{-}G\text{-}F/wt}$ vs *App* $^{NL\text{-}G\text{-}F/NL\text{-}G\text{-}F}$: t(5.323)=-2.125, P=0.084, 95% CI:-1.654, 0.142

Supplementary Table 6. Detailed results of the statistical analyses in Supplementary Figure 2.

Supplementary Figure number	Sample size (n)	Games-Howell
2A	4-month-old mice: WT: n= 13 mice; *App* $^{NL\text{-}G\text{-}F/wt}$: n= 17 mice; *App* $^{NL\text{-}G\text{-}F/NL\text{-}G\text{-}F}$: n= 8 mice; 9-month-old mice: WT: n= 10 mice; *App* $^{NL\text{-}G\text{-}F/wt}$: n= 20 mice; *App* $^{NL\text{-}G\text{-}F/NL\text{-}G\text{-}F}$: n= 16 mice	4 months: WT vs App $^{NL\text{-}G\text{-}F/wt}$: t(25.723)=1.984, *P*=0.137, 95% CI: -9.500, 84.445 WT vs *App* $^{NL\text{-}G\text{-}F/NL\text{-}G\text{-}F}$: t(10.989)=0.926, *P*=0.636, 95% CI: -37.950, 77.530 *App* $^{NL\text{-}G\text{-}F/wt}$ vs *App* $^{NL\text{-}G\text{-}F/NL\text{-}G\text{-}F}$: t(16.873)=0.714, *P*=0.759, 95% CI: -81.241, 45.880 9 months: WT vs *App* $^{NL\text{-}G\text{-}F/wt}$: t(20.049)=0.015, *P*=1.000, 95% .CI: -100.665, 101.831 WT vs *App* $^{NL\text{-}G\text{-}F/NL\text{-}G\text{-}F}$: t(15.506)=0.216, *P*=0.960, 95% CI: -102.842, 87.008 *App* $^{NL\text{-}G\text{-}F/wt}$ vs *App* $^{NL\text{-}G\text{-}F/NL\text{-}G\text{-}F}$: t(33.277)=0.272, *P*=0.938, 95% CI: -85.074, 68.074
2B	4-month-old mice: WT: n= 13 mice; *App* $^{NL\text{-}G\text{-}F/wt}$: n= 17 mice; *App* $^{NL\text{-}G\text{-}F/NL\text{-}G\text{-}F}$: n= 8 mice; 9-month-old mice: WT: n= 10 mice; *App* $^{NL\text{-}G\text{-}F/wt}$: n= 20 mice; *App* $^{NL\text{-}G\text{-}F/NL\text{-}G\text{-}F}$: n= 16 mice	4 months: WT vs *App* $^{NL\text{-}G\text{-}F/wt}$: t(20.308)=0.995, *P*=0.588, 95% CI: -795.548, 346.007 WT vs *App* $^{NL\text{-}G\text{-}F/NL\text{-}G\text{-}F}$: t(18.357)=0.118, *P*=0.992, 95% CI: -700.661, 638.860 *App* $^{NL\text{-}G\text{-}F/wt}$ vs *App* $^{NL\text{-}G\text{-}F/NL\text{-}G\text{-}F}$: t(13.236)=0.911, *P*=0.643, 95% CI: -366.966, 754.706 9 months: WT vs *App* $^{NL\text{-}G\text{-}F/wt}$: t(19.748)=0.341, *P*=0.938, 95% CI: -530.168, 404.363 WT vs *App* $^{NL\text{-}G\text{-}F/NL\text{-}G\text{-}F}$: t(17.685)=0.926, *P*=0.631, 95% CI: -622.349, 291.345 *App* $^{NL\text{-}G\text{-}F/wt}$ vs *App* $^{NL\text{-}G\text{-}F/NL\text{-}G\text{-}F}$: t(33.972)=0.669, *P*=0.783, 95% CI: -478.625, 273.426

Supplementary Table 7. Detailed results of the statistical analyses in Supplementary Figure 3.

Supplementary Figure number	Sample size (n)	Mixed ANOVA	Games-Howell
3A from 5-month-old	WT: n= 12 mice; *App* $^{NL\text{-}G\text{-}F/wt}$: n= 11 mice; *App* $^{NL\text{-}G\text{-}F/NL\text{-}G\text{-}F}$: n= 8 mice	Age: F(1,28)= 0.004, P=0.951 Age*genotype: F(2,28)= 1.686, P=0.204 genotype : F(2,28)= 1.906, P=0.168	n.a.
3A from 7-month-old mice	WT: n= 10 mice; *App* $^{NL\text{-}G\text{-}F/wt}$: n= 12 mice; *App* $^{NL\text{-}G\text{-}F/NL\text{-}G\text{-}F}$: n= 13 mice	Age: F(2,64)= 21.071, P=0.000 Age*genotype: F(4,64)= 0.935, P=0.450 genotype : F(2,32)= 0.724, P=0.493	n.a.